Astrophysical Gyrokinetics: Basic Equations and Linear Theory

Gregory G. Howes¹, Steven C. Cowley², William Dorland³, Gregory W. Hammett⁴, Eliot Quataert¹, and Alexander A. Schekochihin⁵

ghowes@astro.berkeley.edu

ABSTRACT

Magnetohydrodynamic (MHD) turbulence is encountered in a wide variety of astrophysical plasmas, including accretion disks, the solar wind, and the interstellar and intracluster medium. On small scales, this turbulence is expected to be highly anisotropic with frequencies small compared to the ion cyclotron frequency. For a number of applications, the small scale perturbations are also collisionless, so a kinetic treatment of the turbulence is desirable. We show that this anisotropic turbulence is well described by a low frequency expansion of the kinetic theory called gyrokinetics. This paper is the first in a series to examine turbulent astrophysical plasmas in the gyrokinetic limit. We derive and explain the nonlinear gyrokinetic equations and explore the linear properties of gyrokinetics as a prelude to nonlinear simulations. The linear dispersion relation for gyrokinetics is obtained and its solutions are compared to those of hot plasma kinetic theory. These results are used to validate the performance of the gyrokinetic simulation code GS2 in the parameter regime relevant for astrophysical plasmas. New results on global energy conservation in gyrokinetics are also derived. We briefly outline several of the problems to be addressed by future nonlinear simulations, including particle heating by turbulence in hot accretion flows and in the solar wind, the magnetic and electric field power spectra in the solar wind, and the origin of small-scale density fluctuations in the interstellar medium.

Subject headings: Gyrokinetics — methods: numerical — turbulence: magnetic, dissipation

¹Department of Astronomy, 601 Campbell Hall, University of California, Berkeley, CA 94720

²Department of Physics and Astronomy, University of California, Los Angeles, CA 90095-1547 and Blackett Laboratory, Imperial College, London, SW1 2BW

³Center for Scientific Computing and Mathematical Modeling, University of Maryland, College Park, Maryland, 20742

⁴Princeton Plasma Physics Laboratory, P.O. Box 451, Princeton, NJ 08543

⁵DAMTP, University of Cambridge, Cambridge CB3 0WA, UK

1. Introduction

The Goldreich and Sridhar (1995) (hereafter GS) theory of MHD turbulence (see also Sridhar and Goldreich 1994; Goldreich and Sridhar 1997; Lithwick and Goldreich 2001) in a mean magnetic field predicts that the energy cascades primarily perpendicular to the local field, with $k_{\perp} \gg k_{\parallel}$, as schematically shown in Figure 1 (see also earlier work by Montgomery and Turner 1981; Shebalin et al. 1983; Higdon 1984, 1986). Numerical simulations of magnetized turbulence with a mean field support the GS model of anisotropic MHD turbulence (Maron and Goldreich 2001; Cho et al. 2002). In situ measurements of turbulence in the solar wind (Belcher and Davis 1971; Matthaeus et al. 1990; Goldstein et al. 1995; Leamon et al. 1998) and observations of interstellar scintillation (Wilkinson et al. 1994) also provide evidence for significant anisotropy.

In many astrophysical environments, small-scale perturbations in the MHD cascade have (parallel) wavelengths much smaller than, or at least comparable to, the mean free path of ions, electrons, and neutrals, implying that the turbulent dynamics should be calculated using kinetic theory. As a result of the intrinsic anisotropy of MHD turbulence, the small-scale perturbations also have frequencies well below the ion cyclotron frequency, $\omega \ll \Omega_i$, even when the perpendicular wavelengths are comparable to the ion gyroradius (see Figure 1). Anisotropic MHD turbulence in plasmas with weak collisionality can be described by a system of equations called gyrokinetics.

Particle motion in the small-scale turbulence is dominantly the cyclotron motion about the unperturbed field lines. Gyrokinetics exploits the time-scale separation ($\omega \ll \Omega_i$) for the electromagnetic fluctuations to eliminate one degree of freedom in the kinetic description, thereby reducing the dimensionality of the problem from 6 to 5 dimensions. It does so by averaging over the fast cyclotron motion of charged particles in the mean magnetic field. The resulting "gyro-kinetic" equations describe charged "rings" moving in the ring averaged electromagnetic fields. By removing one dimension of phase space and the fast cyclotron time-scale, a more computationally efficient treatment of low frequency turbulent dynamics is achieved. The gyrokinetic system is completed by electromagnetic field equations that are obtained by applying the gyrokinetic ordering to Maxwell's equations. The gyrokinetic approximation orders out the fast MHD wave and cyclotron resonant effects, but retains finite Larmor radius effects, collisionless dissipation via the parallel Landau resonance, and collisions. Both the slow MHD wave and the Alfvén wave are captured by the gyrokinetics, though the former is damped below the scale of the ion mean free path (Barnes 1966; Foote and Kulsrud 1979).

Linear (Rutherford and Frieman 1968; Taylor and Hastie 1968; Catto 1978; Antonsen and Lane 1980; Catto et al. 1981) and nonlinear gyrokinetic theory (Frieman and Chen

1982; Dubin et al. 1983; Hahm et al. 1988) has proven to be a valuable tool in the study of laboratory plasmas. It has been extensively employed to study the development of turbulence driven by micro-instabilities, e.g., ion and electron temperature gradient instabilities (Dorland et al. 2000; Jenko et al. 2000; Rogers et al. 2000; Jenko et al. 2001; Jenko and Dorland 2001, 2002; Candy et al. 2004). For these applications, the structure of the mean equilibrium field and the mean gradients in temperature and density are critical. Thus, the full gyrokinetic equations allow for a spatially varying mean (equilibrium) magnetic field, temperature, and density. In an astrophysical plasma, these instabilities are unlikely to be as important as the MHD turbulence produced by violent large scale events or instabilities. Thus, our goal is to use gyrokinetics to describe the MHD turbulence on small scales (as depicted in Fig. 1). For this application the variation of the large scale field, temperature, and density is unimportant. We therefore consider gyrokinetics in a uniform equilibrium field with no mean temperature or density gradients.

This is the first in a series of papers to apply gyrokinetic theory to the study of turbulent astrophysical plasmas. In this paper, we derive the equations of gyrokinetics in a uniform equilibrium field and explain their physical meaning. We also derive and analyze the linear gyrokinetic dispersion relation in the collisionless regime. Future papers will present analytical reductions of the gyrokinetic equations in various asymptotic limits (Schekochihin et al. 2006) and nonlinear simulations applied to specific astrophysical problems (for a preliminary report, see Dorland et al. 2006). These simulations use the gyrokinetic simulation code GS2—as part of our continuing validation of GS2, we demonstrate here that it accurately reproduces the frequencies and damping rates of the linear modes.

The remainder of this paper is organized as follows. In §2, we present the gyrokinetic system of equations, giving a physical interpretation of the various terms and a detailed discussion of the gyrokinetic approximation. A derivation of the gyrokinetic equations in the limit of a uniform, mean magnetic field with no mean temperature or density gradients is presented in Appendix A. Appendix B contains the first published derivation of the long-term transport and heating equations that describe the evolution of the equilibrium plasma. In Appendix C, we derive the linear, collisionless dispersion relation for gyrokinetics. In §3, we compare this dispersion relation with that of hot plasma theory and with numerical results from the gyrokinetic simulation code GS2. We also discuss the effect of collisions on collisionless damping rates (§3.4) and illustrate the limits of applicability of the gyrokinetic approximation (§3.5). Appendix D contains analytical approximations for the frequency and damping rate of Alfvén waves in several limits. Finally, §4 summarizes our results and discusses several potential astrophysical applications of gyrokinetics. Definitions adopted for plasma parameters in this paper are given in Table 1.

2. Gyrokinetics

In this section we describe the gyrokinetic approximation and present the gyrokinetic equations themselves in a simple and physically motivated manner (the details of the derivation are given in the Appendices). To avoid obscuring the physics with the complexity of gyrokinetics in full generality, we treat here the simplified case of a plasma in a periodic box with a straight, uniform mean magnetic field, $\mathbf{B}_0 = B_0 \hat{\mathbf{z}}$, and a spatially uniform equilibrium distribution function, $\nabla F_0 = 0$ (the slab limit). This case is also of most direct astrophysical relevance because the gradients in the ambient plasma are small and generally dynamically unimportant on length scales comparable to the ion gyroradius.

2.1. The Gyrokinetic Approximation and Ordering

Several approximations must be satisfied for the gyrokinetic equations to be applicable. The most basic are weak coupling, small fluctuations, and strong magnetization. We begin by making the standard weak coupling assumption of plasma physics: $n_{0e}\lambda_{De}^3 \gg 1$, where n_{0e} is the electron number density and λ_{De} is the electron Debye length. This approximation allows the use of the Fokker-Planck equation to describe the kinetic evolution of plasma species.

The condition of strong magnetization for gyrokinetics means that the ion Larmor radius ρ_i must be small with respect to the macroscopic length scale of the equilibrium plasma L and that the frequency of fluctuations ω must be small compared to the ion cyclotron frequency Ω_i ,

$$\rho_i \ll L \quad \text{and} \quad \omega \ll \Omega_i.$$
(1)

The slow time-scale assumption ($\omega \ll \Omega_i$) allows one to average over the Larmor orbits of particles, one of the key simplifications in gyrokinetic theory. Note that the assumption of strong magnetization does not require $\beta \ll 1$, where the plasma β is the ratio of the thermal to the magnetic pressure, $\beta = 8\pi p/B^2$. A high β plasma can satisfy this constraint as long as the ion Larmor radius is small compared to the gradients of the equilibrium system. In most astrophysical contexts, even a very weak magnetic field meets this requirement.

To derive the gyrokinetic equations, we order the disparate time and length scales in the problem to separate fluctuating and equilibrium quantities. The remainder of this section defines this formal ordering and describes some simple consequences that follow from it. Two length scales are characteristic of gyrokinetics: the large length scale characteristic of the parallel wavelength, l_0 ; and the small length scale, the ion Larmor radius ρ_i . Their ratio

defines the fundamental expansion parameter ϵ used in the formal ordering:

$$\epsilon \equiv \frac{\rho_i}{l_0} \ll 1. \tag{2}$$

There are three relevant time-scales, or frequencies, of interest. The fast time-scale is given by the ion cyclotron frequency Ω_i . The distribution function and the fields are assumed to be stationary on this time-scale. The intermediate time-scale is characterized by the frequency of the turbulent fluctuations, $\omega \sim v_{th_i}/l_0 \sim \mathcal{O}(\epsilon\Omega_i)$. The slow time-scale is connected to the rate of heating in the system, $1/t_{heat} \sim \epsilon^2 v_{th_i}/l_0 \sim \mathcal{O}(\epsilon^3\Omega_i)$.

The distribution function f and magnetic and electric fields \mathbf{B} and \mathbf{E} are split into equilibrium parts (denoted with a subscript 0) that vary at the slow heating rate and fluctuating parts (denoted with δ and a subscript indicating the order in ϵ) that vary at the intermediate frequency ω :

$$f(\mathbf{r}, \mathbf{v}, t) = F_0(\mathbf{v}, t) + \delta f_1(\mathbf{r}, \mathbf{v}, t) + \delta f_2(\mathbf{r}, \mathbf{v}, t) + \cdots,$$
(3)

$$\mathbf{B}(\mathbf{r},t) = \mathbf{B}_0 + \delta \mathbf{B}(\mathbf{r},t)$$
 and $\mathbf{E}(\mathbf{r},t) = \delta \mathbf{E}(\mathbf{r},t)$. (4)

We orient our coordinates so that $\mathbf{B}_0 = B_0 \hat{\mathbf{z}}$.

Having defined our notation and the ordering parameter, we now list, in full, the gyrokinetic ordering assumptions.

- Small fluctuations about equilibrium. Fluctuating quantities are formally of order ϵ in the gyrokinetic expansion, $\delta f_1/F_0 \sim |\delta \mathbf{B}|/B_0 \sim |c\delta \mathbf{E}|/(v_{th_i}B_0) \sim \mathcal{O}(\epsilon)$. Note that although the gyrokinetic ordering implies $\delta B \ll B_0$, the theory is fully (strongly) nonlinear.
- Slow time-scale variation of the equilibrium. The equilibrium varies on the heating time-scale, i.e., $(\partial F_0/\partial t)/F_0 \sim \mathcal{O}(1/t_{heat}) \sim \mathcal{O}(\epsilon^2 v_{th_i}/l_0)$. Derivations for laboratory plasmas (Frieman and Chen 1982) have included a large-scale $(\mathcal{O}(1/l_0))$ spatial variation of the equilibrium $(F_0 \text{ and } \mathbf{B}_0)$ —this we omit. The slow-time-scale evolution of the equilibrium, however, is treated for the first time here.
- Intermediate time-scale variation of fluctuating quantities. The variation of the fluctuating quantities occurs on the intermediate time-scale $(\partial \delta f/\partial t)/\delta f \sim (\partial \delta \mathbf{B}/\partial t)/\delta \mathbf{B} \sim (\partial \delta \mathbf{E}/\partial t)/\delta \mathbf{E} \sim \mathcal{O}(v_{th_i}/l_0) \sim \mathcal{O}(\omega)$.
- Intermediate time-scale collisions. The collision rate in gyrokinetics is ordered to act on the intermediate time-scale $\nu \sim \mathcal{O}(v_{th_i}/l_0) \sim \mathcal{O}(\omega)$. Collisionless dynamics with $\omega > \nu$ are treated correctly as long as $\nu > \epsilon \omega$.

- Small-scale spatial variation of fluctuations across the mean field. Across the mean magnetic field, the fluctuations occur on the microscopic length scale $|\hat{\mathbf{z}} \times \nabla \delta f|/\delta f \sim (|\hat{\mathbf{z}} \times \nabla |\delta \mathbf{B})/\delta \mathbf{B} \sim (|\hat{\mathbf{z}} \times \nabla |\delta \mathbf{E})/\delta \mathbf{E} \sim \mathcal{O}(k_{\perp}) \sim \mathcal{O}(1/\rho_i)$.
- Large-scale spatial variation of fluctuations along the mean field. Along the mean magnetic field the fluctuations occur on the macroscopic length scale $(\hat{\mathbf{z}} \cdot \nabla \delta f)/\delta f \sim (\hat{\mathbf{z}} \cdot \nabla \delta \mathbf{B})/\delta \mathbf{B} \sim (\hat{\mathbf{z}} \cdot \nabla \delta \mathbf{E})/\delta \mathbf{E} \sim \mathcal{O}(k_{\parallel}) \sim \mathcal{O}(1/l_0)$.

With a small fluctuation length-scale across the field and a large fluctuation length-scale along the field, the typical gyrokinetic fluctuation is very anisotropic, with

$$\frac{k_{\parallel}}{k_{\perp}} \equiv \frac{l_{\perp}}{l_{\parallel}} = \frac{\rho_i}{l_0} \sim \mathcal{O}(\epsilon). \tag{5}$$

Figure 2 presents a schematic diagram that depicts the length-scales associated with the gyrokinetic ordering. The typical perpendicular flow velocity, roughly the $\mathbf{E} \times \mathbf{B}$ velocity, is $u_{\perp} \sim c\delta \mathbf{E} \times \mathbf{B}/B_0^2 \sim \mathcal{O}(\epsilon v_{th_i})$. The typical perpendicular fluid displacement is $\sim u_{\perp}/\omega \sim \mathcal{O}(\rho_i)$ and the field line displacement is $\sim \int dl \, \delta \mathbf{B}/B_0 \sim \mathcal{O}(\rho_i)$. Thus, displacements are of order the perpendicular wavelength or eddy size and the fluctuations are fully nonlinear.

Let us now consider the consequences of the gyrokinetic ordering on Maxwell's equations. In Faraday's Law, we find $c\nabla \times \delta \mathbf{E} \sim \mathcal{O}(\epsilon\Omega_i B_0)$, whereas $\partial \delta \mathbf{B}/\partial t \sim \mathcal{O}(\epsilon^2\Omega_i B_0)$; therefore, to dominant order the electric field satisfies $\nabla \times \delta \mathbf{E} = 0$, so the largest part of the electric field is electrostatic. The inductive field is important, however, and is kept. The fields are then most conveniently written in terms of the scalar and vector potentials.

Consider next the Ampère/Maxwell Law. The ordering demands that the curl of the perturbed magnetic field is $\nabla \times \delta \mathbf{B} \sim \mathcal{O}(\epsilon B_0/\rho_i)$ and that the displacement current is $(1/c)\partial\delta\mathbf{E}/\partial t \sim \mathcal{O}(\epsilon B_0 v_{th_i}^2/l_0 c^2)$, so the ratio of the displacement current to the curl of magnetic field is $\mathcal{O}(\epsilon v_{th_i}^2/c^2)$. Hence, in the gyrokinetic limit, we can drop the displacement current and use only the unmodified (pre-Maxwell) form of Ampère's Law.

Finally, we consider the balance of terms in Poisson's Law. The ordering mandates $\nabla \cdot \delta \mathbf{E} \sim \mathcal{O}(\epsilon B_0 v_{th_i}/(c\rho_i))$ and $4\pi (n_{0i}q_i + n_{0e}q_e) \sim \mathcal{O}(\epsilon q n_0)$. The ratio of the divergence of the electric field to the charge density is $\mathcal{O}(v_{th_i}^2/\beta_i c^2)$, where β_i is the ion plasma beta. Therefore, the divergence of the electric field is small (in the limit of non-relativistic ions) and, to dominant order, the charge density is zero; this establishes the condition of quasineutrality. Alternatively, one can say that the divergence of the electric field is small for gyrokinetic perturbations whose wavelengths are long compared to the electron Debye length, λ_{De} .

The GS theory of MHD turbulence conjectures that, on sufficiently small scales, fluctuations always arrange themselves in such a way that the Alfvén time-scale and the nonlinear

decorrelation time-scale (turbulent frequency) are similar at each scale, $\omega \sim k_{\parallel}v_{A} \sim k_{\perp}u_{\perp}$ (this is known as the critical balance). A modification of Kolmogorov (1941) dimensional theory based on this additional assumption then leads to the scaling $u_{\perp} \sim U(k_{\perp}L)^{-1/3}$, where U and L are the velocity and the scale at which the turbulence is driven and it is assumed, for simplicity, that the critical balance is already satisfied at this scale. For a detailed discussion of these results, we refer the reader to Goldreich and Sridhar's original papers or to a review by Schekochihin and Cowley (2005). Here, we show that the gyrokinetic ordering is manifestly consistent with and, indeed, can be constructed on the basis of the critical balance conjecture. Using the critical balance and the GS scaling of u_{\perp} , we find that the ratio of the turbulent frequency $\omega \sim k_{\perp}u_{\perp}$ to the ion cyclotron frequency is

$$\frac{\omega}{\Omega_i} \sim \frac{U}{v_{th_i}} \left(k_{\perp} \rho_i \right)^{2/3} \left(\frac{\rho_i}{L} \right)^{1/3}. \tag{6}$$

Similarly, the anisotropy ratio is

$$\frac{k_{\parallel}}{k_{\perp}} \sim \frac{U}{v_{\perp}} (k_{\perp} \rho_i)^{-1/3} \left(\frac{\rho_i}{L}\right)^{1/3}.$$
 (7)

Therefore, in the specific case of the GS model of magnetized turbulence, the expansion parameter $\epsilon = (\rho_i/L)^{1/3} = \rho_i/l_0$. One might worry that the power of 1/3 means that the expansion is valid only in extreme circumstances. For astrophysical plasmas, however, ρ_i/L is so small that this is probably not a significant restriction. To take the interstellar medium as a concrete example, $\rho_i \sim 10^8$ cm and $L \sim 100$ pc $\sim 3 \times 10^{20}$ cm (the supernova scale), so $(\rho_i/L)^{1/3} \sim 10^{-4}$. For galaxy clusters, $(\rho_i/L)^{-1/3} \sim 10^{-5}$ (Schekochihin and Cowley 2006), for hot, radiatively inefficient accretion flows around black holes, $(\rho_i/L)^{1/3} \sim 10^{-3}$ (Quataert 1998), and for the solar wind, $(\rho_i/L)^{1/3} \sim 0.02$.

In view of the above discussion, we may formally define the large parallel length scale used in the gyrokinetic ordering as $l_0 = \rho_i^{2/3} L^{1/3}$, where L is the energy injection scale of the turbulence. Physically, this definition means that the large gyrokinetic length-scale is the characteristic parallel length-scale of the turbulent fluctuations in the context of GS turbulence. Note that this means that our assumption of no spatial variation of the equilibrium is, thus, equivalent to assuming that the variation scale of F_0 and \mathbf{B}_0 is $\gg l_0$ —this is satisfied, e.g., for the injection scale L.

The gyrokinetic ordering implies that all cyclotron frequency effects and the fast MHD wave have been eliminated from the system. The slow and Alfvén waves are retained, however, and collisionless dissipation of fluctuations occurs via the Landau resonance, through both Landau damping and transit-time damping (Stix 1992). The slow and Alfvén waves are accurately described for arbitrary $k_{\perp}\rho_{i}$, as long as they are anisotropic ($k_{\parallel} \sim \epsilon k_{\perp}$).

Subsidiary ordering of collisions (as long as it does not interfere with the primary gyrokinetic ordering) allows for a treatment of collisionless and/or collisional dynamics. Similarly, subsidiary ordering of the plasma beta allows for both low and high beta plasmas. The gyrokinetic ordering encompasses a large subset of relevant plasma dynamics and is therefore a very useful approximation.

2.2. Coordinates and Ring Averages

Gyrokinetics is most naturally described in guiding center coordinates where the position of a particle \mathbf{r} , the position of its guiding center \mathbf{R} , and the Larmor radius $\boldsymbol{\rho}$ are related by

$$\mathbf{r} = \mathbf{R} + \boldsymbol{\rho} \tag{8}$$

with the Larmor radius defined by

$$\rho = \frac{\hat{\mathbf{z}} \times \mathbf{v}}{\Omega}.\tag{9}$$

The particle velocity can be described by the parallel velocity v_{\parallel} , perpendicular velocity v_{\perp} , and the gyrophase angle θ :

$$\mathbf{v} = v_{\parallel} \hat{\mathbf{z}} + v_{\perp} (\cos \theta \hat{\mathbf{x}} + \sin \theta \hat{\mathbf{y}}). \tag{10}$$

By averaging over the Larmor motion of particles, gyrokinetics describes the evolution of a distribution of rings rather than individual particles. The derivation of the equations requires both a ring average at constant (ring) guiding center \mathbf{R} , defined by

$$\langle a(\mathbf{r}, \mathbf{v}, t) \rangle_{\mathbf{R}} = \frac{1}{2\pi} \oint d\theta \, a(\mathbf{R} - \frac{\mathbf{v} \times \hat{\mathbf{z}}}{\Omega}, \mathbf{v}, t),$$
 (11)

where the θ integration is done keeping \mathbf{R} , v_{\perp} and v_{\parallel} constant, and a ring average at fixed position \mathbf{r} , given by

$$\langle a(\mathbf{R}, \mathbf{v}, t) \rangle_{\mathbf{r}} = \frac{1}{2\pi} \oint d\theta \, a(\mathbf{r} + \frac{\mathbf{v} \times \hat{\mathbf{z}}}{\Omega}, \mathbf{v}, t).$$
 (12)

2.3. The Gyrokinetic Equations

The derivation of the gyrokinetic equations is given in Appendix A. Here we summarize the results and their physical interpretation. Table 2 defines various quantities used in this discussion. From the minus first and zeroth order of the expansion we obtain the form of the distribution function:

$$f_s = F_{0s}(v,t) \exp\left(-\frac{q_s\phi(\mathbf{r},t)}{T_{0s}}\right) + h_s(\mathbf{R}_s, v, v_\perp, t) + \delta f_{2s} + \cdots,$$
(13)

where the equilibrium distribution function is Maxwellian:

$$F_{0s} = \frac{n_{0s}}{\pi^{3/2}} \frac{1}{v_{ths}^3} \exp\left(-\frac{v^2}{v_{ths}^2}\right). \tag{14}$$

The ring distribution $h_s \sim \mathcal{O}(\epsilon F_{0s})$ is part of the first order distribution function. The other first order part comes from the Boltzmann factor $\exp(-\frac{q_s\phi(\mathbf{r},t)}{T_{0s}}) \simeq 1 - q_s\frac{\phi(\mathbf{r},t)}{T_{0s}}$. The ring distribution h_s is a function of the guiding center position \mathbf{R}_s (not the position \mathbf{r}), and it satisfies the **gyrokinetic equation**:

$$\frac{\partial h_s}{\partial t} + v_{\parallel} \hat{\mathbf{z}} \cdot \frac{\partial h_s}{\partial \mathbf{R}_s} + \frac{c}{B_0} \left[\langle \chi \rangle_{\mathbf{R}_s}, h_s \right] - \left\langle \left(\frac{\partial h_s}{\partial t} \right)_{\text{coll}} \right\rangle_{\mathbf{R}_s} = \frac{q_s}{T_{0s}} \frac{\partial \langle \chi \rangle_{\mathbf{R}_s}}{\partial t} F_{0s}. \tag{15}$$

Maxwell's equations become the quasineutrality condition,

$$\sum_{s} \left(-\frac{q_s^2 n_{0s}}{T_{0s}} \phi + q_s \int d^3 \mathbf{v} \langle h_s \rangle_{\mathbf{r}} \right) = 0, \tag{16}$$

the parallel component of Ampère's Law,

$$-\nabla_{\perp}^{2} A_{\parallel} = \sum_{s} \frac{4\pi}{c} q_{s} \int d^{3}\mathbf{v} v_{\parallel} \langle h_{s} \rangle_{\mathbf{r}}, \tag{17}$$

and the perpendicular component of Ampère's Law,

$$\nabla_{\perp} \delta B_{\parallel} = \sum_{s} \frac{4\pi}{c} q_{s} \int d^{3} \mathbf{v} \langle (\hat{\mathbf{z}} \times \mathbf{v}_{\perp}) h_{s} \rangle_{\mathbf{r}}.$$
 (18)

Note that the nonlinear terms in the gyrokinetic equation (15) enter through the Poisson bracket term; this term can be written in a more physically illuminating "velocity" form as

$$\frac{c}{B_0} \left[\langle \chi \rangle_{\mathbf{R}_s}, h_s \right] = -\frac{c}{B_0} \left(\frac{\partial \langle \chi \rangle_{\mathbf{R}_s}}{\partial \mathbf{R}_s} \times \hat{\mathbf{z}} \right) \cdot \frac{\partial h_s}{\partial \mathbf{R}_s}. \tag{19}$$

The second and third terms on the left-hand side of the gyrokinetic equation (15) can then be written in terms of the ring velocity in the form $\langle d\mathbf{R}_s/dt\rangle_{\mathbf{R}_s} \cdot \partial h_s/\partial \mathbf{R}_s$, where, using the definition of χ , the ring velocity is

$$\left\langle \frac{d\mathbf{R}_{s}}{dt} \right\rangle_{\mathbf{R}_{s}} = v_{\parallel} \hat{\mathbf{z}} - \frac{c}{B_{0}} \frac{\partial \langle \chi \rangle_{\mathbf{R}_{s}}}{\partial \mathbf{R}_{s}} \times \hat{\mathbf{z}}$$

$$= v_{\parallel} \hat{\mathbf{z}} - \frac{c}{B_{0}} \frac{\partial \langle \phi \rangle_{\mathbf{R}_{s}}}{\partial \mathbf{R}_{s}} \times \hat{\mathbf{z}} + \frac{\partial \langle v_{\parallel} A_{\parallel} \rangle_{\mathbf{R}_{s}}}{\partial \mathbf{R}_{s}} \times \left(\frac{\hat{\mathbf{z}}}{B_{0}}\right) + \frac{\partial \langle \mathbf{v}_{\perp} \cdot \mathbf{A}_{\perp} \rangle_{\mathbf{R}_{s}}}{\partial \mathbf{R}_{s}} \times \left(\frac{\hat{\mathbf{z}}}{B_{0}}\right) (20)$$

We also note that the ring averaged rate of change of the total particle energy is

$$\left\langle \frac{d}{dt} \left(\frac{1}{2} m_s v^2 + q_s \phi \right) \right\rangle_{\mathbf{R}_s} = q_s \frac{\partial \langle \chi \rangle_{\mathbf{R}_s}}{\partial t}. \tag{21}$$

S	Particle species
m_s	Particle mass
n_{0s}	Number density
q_s	Particle charge
T_{0s}	Temperature (in units of energy)
c	Speed of light
$\mathbf{B_0} = B_0 \hat{\mathbf{z}}$	Mean magnetic field
$F_{0s}(v,t)$	Maxwellian equilibrium distribution function
$v_{th_s} = (2T_{0s}/m_s)^{1/2}$	Thermal velocity
$\Omega_s = q_s B_0 / (m_s c)$	Cyclotron frequency (carries sign of q_s)
$\rho_s = v_{th_s}/\Omega_s$	Larmor radius

Table 1: Definitions of all quantities and characteristic values associated with each plasma species.

h_s	Gyrokinetic perturbed distribution function
v	Velocity $\mathbf{v} = v_{\parallel} \hat{\mathbf{z}} + \mathbf{v}_{\perp}$
ϕ	Scalar potential
A_{\parallel}	Parallel component of vector potential
δB_{\parallel}	Parallel component of perturbed magnetic field
χ	Gyrokinetic potential $\chi = \phi - \mathbf{v} \cdot \mathbf{A}/c$
r	Particle position
\mathbf{R}_s	Guiding center position
$\langle \rangle_{\mathbf{r}}$	Ring average at constant position
$\langle angle_{\mathbf{R}_s}$	Ring average at constant guiding center
[,]	Poisson bracket defined by $[u, v] = \frac{\partial u}{\partial x} \frac{\partial v}{\partial y} - \frac{\partial u}{\partial y} \frac{\partial v}{\partial x}$
$\left(\frac{\partial h_s}{\partial t}\right)_{\text{coll}}$	Collision term

Table 2: Definitions of all quantities in the system of nonlinear gyrokinetic equations given by equations (15)–(18).

A simple physical interpretation can be given for the gyrokinetic equation (15). By taking the ring average at constant guiding center \mathbf{R}_s , as defined in §2.2, the gyrokinetic equation describes the evolution of a distribution of rings h_s ; each term corresponds to a physical influence on this ring distribution function. Let us consider the physical meaning of each term of the gyrokinetic equation (15) written using equation (20):

- $v_{\parallel}\hat{\mathbf{z}}\cdot(\partial h_s/\partial\mathbf{R}_s)$ is the motion of the ring along the unperturbed magnetic field.
- $-\frac{c}{B_0}(\partial \langle \phi \rangle_{\mathbf{R}_s}/\partial \mathbf{R}_s) \times \hat{\mathbf{z}} \cdot (\partial h_s/\partial \mathbf{R}_s)$ is the ring averaged $\mathbf{E} \times \mathbf{B}$ drift.
- $(\partial \langle v_{\parallel} A_{\parallel} \rangle_{\mathbf{R}_s} / \partial \mathbf{R}_s) \times (\hat{\mathbf{z}}/B_0) \cdot (\partial h_s / \partial \mathbf{R}_s)$ is the correction to the parallel motion due to motion along the ring averaged tilted perturbed field line $(\langle \delta \mathbf{B}_{\perp} \rangle_{\mathbf{R}_s})$.
- $(\partial \langle \mathbf{v}_{\perp} \cdot \mathbf{A}_{\perp} \rangle_{\mathbf{R}_s} / \partial \mathbf{R}_s) \times (\hat{\mathbf{z}}/B_0) \cdot (\partial h_s / \partial \mathbf{R}_s)$ is the ring averaged ∇B drift due to the perturbed magnetic field.
- $-\left\langle \left(\frac{\partial h_s}{\partial t}\right)_{\text{coll}}\right\rangle_{\mathbf{R}_s}$ is the (linearized) effect of collisions on the perturbed ring distribution function.
- $(q_s/T_{0s})(\partial \langle \chi \rangle_{\mathbf{R}_s}/\partial t)F_{0s}$ is the effect of collisionless work done on the rings from the fields by wave-ring interactions.

Here we have referred to the ring averaged versions of the more familiar guiding center drifts. Figure 2 shows the drift of the ring along and across the magnetic field.

2.4. Heating in Gyrokinetics

The set of equations given in the previous section determines the evolution of the perturbed ring distribution and the field fluctuations on the intermediate time-scale characteristic of the turbulent fluctuations. To obtain the evolution of the distribution function F_0 on the long heating time-scale (with characteristic frequency of order $\mathcal{O}(\epsilon^2 v_{th_i}/l_0)$), we must continue the expansion to order ϵ^2 . Appendix B details the derivation of the particle transport and heating equations for our homogeneous equilibrium, including the equation defining the conservation of energy in externally driven systems (e.g., "forced" turbulence). In an inhomogeneous plasma, turbulent diffusion, or transport, also enters at this "transport" time-scale.

In the homogeneous case, there is no particle transport on the long time-scale,

$$\frac{dn_{0s}}{dt} = 0. (22)$$

The evolution of the temperature T_{0s} of species s on the transport time-scale is

$$\frac{3}{2}n_{0s}\frac{dT_{0s}}{dt} = \int \frac{d^{3}\mathbf{R}_{s}}{V} \int d^{3}\mathbf{v}q_{s}\frac{\overline{\partial\langle\chi\rangle_{\mathbf{R}_{s}}}h_{s} + n_{0s}\nu_{E}^{sr}(T_{0r} - T_{0s})$$

$$= -\int \frac{d^{3}\mathbf{r}}{V} \int d^{3}\mathbf{v}\frac{T_{0s}}{F_{0s}} \overline{\langle h_{s}\left(\frac{\partial h_{s}}{\partial t}\right)_{\text{coll}}\rangle_{\mathbf{R}_{s}}} + n_{0s}\nu_{E}^{sr}(T_{0r} - T_{0s}). \tag{23}$$

The overbar represents a medium time average over Δt as defined by equation (B1), where $1/\omega \ll \Delta t \ll 1/(\omega \epsilon^2)$. The second term on the right-hand side (proportional to ν_E^{sr}) corresponds to the collisional energy exchange (Huba 2004) between species r and s^1 . In the first expression for the heating, the \mathbf{v} integration is done at constant \mathbf{R}_s , then the \mathbf{R}_s integration is done over the whole system volume V. In the second expression, the \mathbf{v} integration is done at fixed \mathbf{r} , then the \mathbf{r} integration is over the whole system. It is clear from the second form of the heating rate that the heating is ultimately collisional, as it must be since entropy only increases due to collisions. When the collisionality is small, $\nu \ll \omega$, the heating is due to the collisionless Landau damping in the sense that the distribution function h_s develops small-scale structure in velocity space, with velocity scales $\Delta \mathbf{v} \sim \mathcal{O}(\nu^{1/2})$. Collisions smooth these small scales at the rate $\nu v_{th_i}^2/(\Delta v)^2 \sim \omega$, so that the heating rate (given by the second expression in equation (23)) becomes asymptotically independent of ν in the collisionless limit (see Figure 7 and discussion in §3.4).

In the homogeneous case, turbulence will damp away unless driven. Therefore, to study steady state turbulence in a homogeneous case, we must drive the system. In our simulations, we have chosen to do this via a driven antenna current \mathbf{J}_a in Ampère's law—i.e., we add the parallel and perpendicular components of \mathbf{J}_a to the right hand sides of equations (17)–(18). The work done by the antenna satisfies

$$\sum_{s} \frac{3}{2} n_{0s} \frac{dT_{0s}}{dt} = -\int \frac{d^3 \mathbf{r}}{V} \overline{\mathbf{J}_a \cdot \mathbf{E}}.$$
 (24)

It is clear that the energy input from the driving antenna is dissipated as heat in the plasma species. The lesson of equation (23) is that this heat is produced by entropy-increasing

¹We have been cavalier about treating the collision operator up to this point. The characteristic frequency of the interspecies collisional heat exchange $\nu^{ei} \sim \nu^{ii} \sqrt{m_e/m_i} (T_{0i} - T_{0e})/T_{0e} = \mathcal{O}(\nu^{ii} \sqrt{m_e/m_i} \Delta T_0/T_0)$, where ΔT_0 is the temperature difference between species. The characteristic frequency of the long time-scale heating is $\mathcal{O}(\omega\epsilon^2)$; for the two terms on the right-hand side of equation (23) to be formally of the same order, we must specify that $\nu^{ii} \sqrt{m_e/m_i} \Delta T_0/T_0 = \mathcal{O}(\omega\epsilon^2)$. This ordering not only means that the zeroth-order distribution function is a Maxwellian but also provides greater flexibility in ordering the collisionality relative to the intermediate time-scale of the fluctuations. We ignore this technical detail here—in most cases, the second term on the right-hand side of equation (23) is small compared to the first term, allowing a large temperature difference between species to be maintained.

collisions. A related discussion of entropy production in the collisionless limit is given by Krommes and Hu (1994).

2.5. Linear Collisionless Dispersion Relation

The derivation of the linear dispersion relation from the set of gyrokinetic equations (15)–(18) requires several steps. First, the nonlinear terms contained in the Poisson bracket and the collision term are dropped from the gyrokinetic equation (15) leaving the linear, collisionless gyrokinetic equation

$$\frac{\partial h_s}{\partial t} + v_{\parallel} \frac{\partial h_s}{\partial z} = \frac{q_s}{T_{0s}} F_{0s} \frac{\partial \langle \chi \rangle_{\mathbf{R}_s}}{\partial t}.$$
 (25)

Next, assuming that the electromagnetic fields and the gyrokinetic distribution function can be expressed as plane waves, the ring averages appearing in the equations can be written as multiplications by Bessel functions. The gyrokinetic equation can then be solved algebraically for the distribution function. This solution for the distribution function is substituted into equations (16)–(18) and the integration over velocity is performed using the plasma dispersion function to simplify the parallel velocity integrals and modified Bessel functions to express the perpendicular velocity integrals. The details of these steps are given in Appendix C.

The resulting set of algebraic equations for the electromagnetic fields can be solved, yielding the dispersion relation for linear, collisionless gyrokinetics

$$\left[\frac{\alpha_i A}{\overline{\omega}^2} - AB + B^2\right] \left[\frac{2A}{\beta_i} - AD + C^2\right] = \left[AE + BC\right]^2, \tag{26}$$

where we have used the definitions

$$A = \sum_{s} \frac{T_{0i}}{T_{0s}} [1 + \Gamma_0(\alpha_s) \xi_s Z(\xi_s)], \tag{27}$$

$$B = \sum_{s} \frac{T_{0i}}{T_{0s}} [1 - \Gamma_0(\alpha_s)], \tag{28}$$

$$C = \sum_{s} \frac{q_i}{q_s} \Gamma_1(\alpha_s) \xi_s Z(\xi_s), \tag{29}$$

$$D = \sum_{s} \frac{T_{0s}}{T_{0i}} \Gamma_2(\alpha_s) \xi_s Z(\xi_s), \tag{30}$$

$$E = \sum_{s} \frac{q_i}{q_s} \Gamma_1(\alpha_s), \tag{31}$$

$$\xi_s = \frac{\omega}{|k_{\parallel}| v_{th_s}},\tag{32}$$

$$\alpha_s = \frac{k_\perp^2 \rho_s^2}{2},\tag{33}$$

and

$$\overline{\omega} = \frac{\omega}{k_{\parallel} v_A}.\tag{34}$$

The functions $\Gamma_0(\alpha_s)$, $\Gamma_1(\alpha_s)$, and $\Gamma_2(\alpha_s)$ and the plasma dispersion function $Z(\xi_s)$ are defined in Appendix C. The complex eigenvalue solution $\overline{\omega}$ to the equation (26) depends on three dimensionless parameters: the ratio of the ion Larmor radius to the perpendicular wavelength, $k_{\perp}\rho_i$; the ion plasma beta, or the ratio of ion thermal pressure to magnetic pressure, β_i ; and the ion to electron temperature ratio, T_{0i}/T_{0e} . Therefore, we can express the solution of the gyrokinetic dispersion relation as $\overline{\omega} = \overline{\omega}_{GK}(k_{\perp}\rho_i, \beta_i, T_{0i}/T_{0e})$.

2.6. Large Wavelength Limit

To gain more physical insight into the meaning of the linear, collisionless gyrokinetic dispersion relation, we investigate the limiting behavior at scales large compared to the ion Larmor radius, where the comparison to MHD is more straightforward. These are not new results, but they are important starting points for the more general results to follow. First, recall the MHD waves in the gyrokinetic anisotropic limit $k_{\parallel} \ll k_{\perp}$:

$$\omega = \pm k_{\parallel} v_A \qquad \text{The Alfv\'en waves,}$$

$$\omega = \pm k_{\parallel} v_A \left(\frac{\gamma \beta}{\gamma \beta + 1}\right)^{1/2} \qquad \text{The slow waves,}$$

$$\omega = \pm k_{\perp} v_A \left(\gamma \beta + 1\right)^{1/2} \qquad \text{The fast magnetosonic waves,}$$

$$\omega = 0 \qquad \text{The entropy mode,}$$
(35)

where γ is the ratio of specific heats. The fast magnetosonic waves have been ordered out of gyrokinetics because, when $k_{\perp}\rho_i \sim 1$, their frequency is of order the cyclotron frequency Ω_i . The removal of the fast waves is achieved by balancing the perpendicular plasma pressure with the magnetic field pressure (see equation (A27)). Here we are concerned with the Alfvén and slow waves in the collisionless limit.

The left-hand side of equation (26) contains two factors. We will demonstrate that the first factor corresponds to the Alfvén wave solution, the second to the slow wave solution.

The right-hand side of equation (26) represents a finite Larmor radius coupling between the Alfvén and slow waves that is only important at finite ion Larmor radius, $k_{\perp}\rho_i \geq 1$.

In the large-scale limit $k_{\perp}^2 \rho_i^2 \ll 1$, or $\alpha_i \ll 1$, we can expand the functions $\Gamma_0(\alpha_s)$, $\Gamma_1(\alpha_s)$, and $\Gamma_2(\alpha_s)$ as follows: $\Gamma_0(\alpha_s) \simeq 1 - \alpha_s$, $\Gamma_1(\alpha_s) \simeq 1 - 3\alpha_s/2$, and $\Gamma_2(\alpha_s) \simeq 2 - 3\alpha_s$. The dispersion relation in this limit simplifies to

$$\left[\frac{1}{\overline{\omega}^2} - 1\right] \left[\frac{2}{\beta_i} - D + \frac{C^2}{A}\right] = 0. \tag{36}$$

The first factor leads to the familiar Alfvén wave dispersion relation:

$$\omega = \pm k_{\parallel} v_A. \tag{37}$$

Thus the Alfvén wave dispersion relation in the $\rho_i \to 0$ limit is unchanged from the MHD result. This is expected (and well known) since this wave involves no motions or forces parallel to the mean magnetic field. The wave is undamped and the plasma dispersion function (which contains the wave-particle resonance effects) does not appear in this branch of the dispersion relation. To higher order in $k_{\perp}\rho_i$, however, the Alfvén wave is weakly damped; taking the large beta result ($\beta_i \gg 1$), derived in Appendix D.1, we find the damping of the Alfvén wave in the limit $\alpha_i \ll 1$ is given by

$$\frac{\gamma}{\omega} = -\frac{9}{16} \frac{k_\perp^2 \rho_i^2}{2} \sqrt{\frac{\beta_i}{\pi}}.$$
 (38)

The second factor in equation (36) represents the slow wave solution of the dispersion relation. The slow wave involves motions and forces along the magnetic field line and, unlike in the MHD collisional limit, is damped significantly (Barnes 1966). The plasma dispersion function enters through A, C, and D; to further simplify the expression for the slow wave, we must take the low and high beta limits.

In the low beta limit, $\sqrt{\beta_i} \ll 1$, we shall see that the phase velocity of the slow wave is of the order of the sound speed $c_s = (T_{0e}/m_i)^{1/2}$. The electrons then move faster than the wave because $v_{th_e}/c_s = (2m_i/m_e)^{1/2} \gg 1$. In this limit, we can drop all terms involving electron plasma dispersion functions. If we further assume that $T_{0e} \gg T_{0i}$, then the ions are moving slower than the sound speed, $v_{th_i}/c_s = (2T_{0i}/T_{0e})^{1/2} \ll 1$, so we have $\xi_i \gg 1$. Expanding the plasma dispersion function in this limit (Fried and Conte 1961) gives

$$\xi_i Z(\xi_i) \simeq i\sqrt{\pi}\xi_i e^{-\xi_i^2} - 1 + \frac{1}{2\xi_i^2}.$$
 (39)

The slow wave portion of equation (36) now reduces to

$$\frac{T_{0i}}{T_{0e}} - \frac{1}{2} \left(\frac{k_{\parallel} v_{th_i}}{\omega} \right)^2 + i \sqrt{\pi} \frac{\omega}{k_{\parallel} v_{th_i}} e^{-(\omega/k_{\parallel} v_{th_i})^2} = 0.$$
 (40)

Assuming weak damping, to be checked later, we can solve for the real frequency and damping rate by expanding this equation about the real frequency. Solving for the real frequency from the real part of equation (40) gives

$$\omega = \pm k_{\parallel} c_s; \tag{41}$$

this is the familiar ion acoustic wave. Solving for the damping gives

$$\frac{\gamma}{\omega} = -\sqrt{\frac{\pi}{8}} \left(\frac{T_{0e}}{T_{0i}}\right)^{3/2} e^{-T_{0e}/2T_{0i}}.$$
(42)

Thus, for $T_{0e}/T_{0i} \gg 1$, we verify that the *a priori* assumptions we made above are valid. This solution agrees with the standard solution for ion acoustic waves (e.g., Krall and Trivelpiece 1986, §8.6.3) in the limit $k^2 \lambda_{De}^2 \ll 1$.

In the large beta limit, $\sqrt{\beta_i} \gg 1$, we expect again that the slow mode is damped (Foote and Kulsrud 1979). In this case, the argument of the plasma dispersion function for the ion terms will be small $\xi_i \ll 1$ (verified by the outcome), and we can use the power series expansion (Fried and Conte 1961)

$$\xi_i Z(\xi_i) \simeq i\sqrt{\pi}\xi_i - 2\xi_i^2 \tag{43}$$

to solve for the complex frequency analytically. The electron terms once again may be dropped, leaving the solution

$$\frac{\omega}{|k_{\parallel}|v_{th_i}} = -\frac{i}{\beta_i\sqrt{\pi}}.\tag{44}$$

This frequency of the slow mode is purely imaginary, so the mode does not propagate and is strictly damped, in agreement with Foote and Kulsrud (1979). Note that ξ_i is indeed small.

In summary, taking the large scale limit, $k_{\perp}\rho_{i}\ll 1$, of the gyrokinetic dispersion relation has shown that it separates neatly into an Alfvén wave mode and a slow wave mode (the fast wave is ordered out by the gyrokinetic approximation). We expect magnetized turbulence that is generated at large, collisional scales (where the MHD approximation is valid) to nonlinearly cascade to smaller scales (Kolmogorov 1941; Goldreich and Sridhar 1995). We have seen here that slow waves are damped by collisionless Landau damping, even in the large-scale limit, $k_{\perp}\rho_{i}\ll 1$. Therefore, as the scale of turbulent motions falls below the mean free path, the slow mode should be effectively damped out, particularly for high β plasmas. The remaining turbulent motions that cascade down to the scale of the ion Larmor radius are expected to be entirely Alfvénic in character (this can, indeed, be rigorously demonstrated; see Schekochihin et al. 2006). In Appendices (D.1) and (D.2) we present the high and low beta limits of the dispersion relation for the Alfvén mode.

2.7. Small Wavelength Limit

At wavelengths small compared to the ion Larmor radius, $k_{\perp}\rho_i \gg 1$, the low frequency dynamics are those of kinetic Alfvén waves (Hasegawa and Chen 1975). It is expected that low frequency Alfvén wave energy cascading to wavelengths smaller than the ion Larmor radius is channeled into this kinetic Alfvén wave branch. The nonlinear turbulent cascade of energy to yet smaller wavelengths continues until the electron Larmor radius is reached, at which point the electromagnetic wave Landau damps on the electrons.

For $k_{\perp}\rho_i \gg 1$, the kinetic Alfvén wave dispersion relation for low and high β limits is given by (Hasegawa and Chen 1975; Kingsep et al. 1990)

$$\omega^{2} = \begin{cases} k_{\parallel}^{2} v_{A}^{2} \left(\frac{1 + T_{0e} / T_{0i}}{2} \right) (k_{\perp} \rho_{i})^{2} & \beta_{i} \ll 1 \\ k_{\parallel}^{2} v_{A}^{2} \frac{(k_{\perp} \rho_{i})^{2}}{\beta_{i}} & \beta_{i} \gg 1 \end{cases}$$
(45)

Here the low beta limit is valid for $m_e/m_i \ll \beta_i \ll 1^2$.

Dropping all ion velocity integrals and all electron plasma dispersion functions allows us to solve for the gyrokinetic dispersion relation in this limit. For the high and low beta limits, at wavelengths larger than the electron Larmor radius, $\alpha_e \ll 1$, the gyrokinetic dispersion relation reproduces equation (45). The corresponding damping rates are

$$\gamma = \begin{cases} -|k_{\parallel}| v_A \frac{(k_{\perp} \rho_i)^2}{4} \sqrt{\frac{\pi}{\beta_i}} \left(\frac{m_e T_{0e}}{m_i T_{0i}} \right)^{1/2} & \beta_i \ll 1 \\ -|k_{\parallel}| v_A \frac{(k_{\perp} \rho_i)^2}{2} \sqrt{\frac{\pi}{\beta_i}} \left[\frac{1}{\sqrt{\pi} (k_{\perp} \rho_i)^3} + \left(\frac{m_e T_{0e}}{m_i T_{0i}} \right)^{1/2} \right] & \beta_i \gg 1 \end{cases}$$
(46)

3. Numerical Results

Gyrokinetic theory is a powerful tool for investigating nonlinear, low frequency kinetic physics. We have performed a thorough check of the gyrokinetic simulation code GS2 against the results of linear collisionless gyrokinetic and linear hot plasma theory. This section presents the results of a suite of linear tests over a wide range of the three relevant parameters: the ratio of the ion Larmor radius to the perpendicular wavelength $k_{\perp}\rho_i$; the ion plasma beta, or the ratio of ion thermal pressure to magnetic pressure, β_i ; and the ion to electron temperature ratio T_{0i}/T_{0e} . We compare the results of three numerical methods: the gyrokinetic simulation code GS2, the linear collisionless gyrokinetic dispersion relation, and the linear hot plasma dispersion relation.

²The region of validity for equation (45) is more strictly $1 \ll k_{\perp} \rho_i \ll \beta_i^{1/2} (m_i/m_e)^{1/2} (T_{0e}/T_{0i})^{1/2}$.

GS2 is a publicly available, widely used gyrokinetic simulation code, developed³ to study low-frequency turbulence in magnetized plasmas (Kotschenreuther et al. 1995; Dorland et al. 2000). The basic algorithm is Eulerian; equations (15)–(18) are solved for the self-consistent evolution of 5-D distribution functions (one for each species) and the electromagnetic fields on fixed spatial grids. All linear terms are treated implicitly, including the field equations (Kotschenreuther et al. 1995). The nonlinear terms are advanced with an explicit, second-order accurate Adams-Bashforth scheme.

Since turbulent structures in gyrokinetics are highly elongated along the magnetic field, GS2 uses field-line-following Clebsch coordinates to resolve such structures with maximal efficiency, in a flux tube of modest perpendicular extent (Beer, Cowley and Hammett 1995). Pseudo-spectral algorithms are used in the spatial directions perpendicular to the field and for the two velocity space coordinate grids (energy $E = v^2/2$ and magnetic moment $\mu = v_{\perp}^2/2B$) for high accuracy on computable 5-D grids. The code offers wide flexibility in simulation geometry, allowing for optimal representation of the complex toroidal geometries of interest in fusion research. For the astrophysical applications pursued here, we require only the simple, periodic slab geometry in a uniform equilibrium magnetic field with no mean temperature or density gradients.

The linear calculations of collisionless wave damping and particle heating presented in this section employed an antenna driving the parallel component of the vector potential A_{\parallel} (this drives a perpendicular perturbation of the magnetic field). The simulation was driven at a given frequency ω_a and wavenumber \mathbf{k}_a by adding the driven component to the left hand side of equation (17). To determine the mode frequency ω and damping rate γ , the driving frequency was swept slowly $(\dot{\omega}_a/\omega_a \ll \gamma)$ through the resonant frequency to measure the Lorentzian response. Fitting the curve of the Lorentzian recovers the mode frequency and damping rate. These damping rates were verified in decaying runs: the plasma was driven to steady state at the resonant frequency $\omega_a = \omega$; then the antenna was shut off and the decay rate of the wave energy measured. The ion to electron heating ratio was determined by driving the plasma to steady state at the resonant frequency $\omega_a = \omega$ and calculating the heating of each species using diagnostics based on both forms of equation (23).

The linear results obtained from GS2 are compared to two sets of analytical solutions:

1. Given the three input parameters $k_{\perp}\rho_i$, β_i , and T_{0i}/T_{0e} , the linear, collisionless gyrokinetic dispersion relation (equation (26)) is solved numerically using a two-dimensional Newton's method root search in the complex frequency plane, obtaining the solution $\overline{\omega}$ =

³Code development continues with support from the Department of Energy's Center for Multiscale Plasma Dynamics.

 $\overline{\omega}_{GK}(k_{\perp}\rho_i,\beta_i,T_{0i}/T_{0e}).$

2. The hot plasma dispersion relation (Stix 1992) is solved numerically (also using a two-dimensional Newton's method root search) for an electron and proton plasma characterized by an isotropic Maxwellian with no drift velocities (Quataert 1998). To obtain accurate results at high $k_{\perp}\rho_i$, it is necessary that the number of terms kept in the sum of Bessel functions appearing in the dispersion relation is about the same as $k_{\perp}\rho_i$. The linear hot plasma dispersion relation depends on five parameters: $k_{\perp}\rho_i$, the ion plasma beta β_i , the ion to electron temperature ratio T_{0i}/T_{0e} , the ratio of the parallel to the perpendicular wavelength k_{\parallel}/k_{\perp} , and the ratio of the ion thermal velocity to the speed of light v_{th_i}/c . Hence, the solution of the hot plasma dispersion function may be expressed as $\overline{\omega} = \overline{\omega}_{HP}(k_{\perp}\rho_i, \beta_i, T_{0i}/T_{0e}, k_{\parallel}/k_{\perp}, v_{th_i}/c)$. The hot plasma theory must reduce to gyrokinetic theory in the limit that $k_{\parallel} \ll k_{\perp}$ and $v_{th_i}/c \ll 1$ —i.e., $\overline{\omega}_{HP}(k_{\perp}\rho_i, \beta_i, T_{0i}/T_{0e}, 0, 0) = \overline{\omega}_{GK}(k_{\perp}\rho_i, \beta_i, T_{0i}/T_{0e})$.

For a wide range of parameters, we present three tests of the codes for verification: §3.1 presents the frequency and damping rate of Alfvén waves; §3.2 compares the ratio of ion to electron heating due to the linear collisionless damping of Alfvén waves; and §3.3 examines the density fluctuations associated with the Alfvén mode when it couples to the compressional slow wave around $k_{\perp}\rho_{i} \sim \mathcal{O}(1)$. The effect of collisions on the collisionless damping rates is discussed in §3.4. The breakdown of gyrokinetic theory in the limit of weak anisotropy $k_{\parallel} \sim k_{\perp}$ and high frequency $\omega \sim \Omega_{i}$ is demonstrated and discussed in §3.5.

3.1. Frequency and Damping Rates

The frequency and collisionless damping rates for the three methods are compared for temperature ratios $T_{0i}/T_{0e}=100$ and $T_{0i}/T_{0e}=1$ and for ion plasma beta values $\beta_i=10,1,0.1,0.01$ over a range of $k_{\perp}\rho_i$ from 0.1 to 100. The temperature ratio $T_{0i}/T_{0e}=100$ is motivated by accretion disk physics and the temperature ratio $T_{0i}/T_{0e}=1$ is appropriate for studies of the interstellar medium and the solar wind. The frequency $\omega=\mathrm{Re}(\omega)$ and damping rate $\gamma=-\mathrm{Im}(\omega)$ are normalized to the Alfvén frequency $k_{\parallel}v_A$. The hot plasma calculations in this section maintain a constant value of $k_{\parallel}/k_{\perp}=0.001$ and $v_{th_i}/c=0.001$, the regime in which hot plasma theory should produce identical results to gyrokinetics. The number of Bessel functions used in the sum for these results was 100, so the results will be accurate for $k_{\perp}\rho_i \leq 100$.

Figure 3 presents the results for the temperature ratio $T_{0i}/T_{0e} = 100$; Figure 4, for the temperature ratio $T_{0i}/T_{0e} = 1$. Hot plasma calculations are denoted by a solid line, gyrokinetic results by a dashed line, and GS2 results by open squares. The results confirm

accurate performance by GS2 over the range of parameters tested.

3.2. Ion and Electron Heating

An important goal of our nonlinear gyrokinetic simulations to be presented in future papers is to calculate the ratio of ion to electron heating in collisionless turbulence. Using a medium time averaged version of equation (B9), the solutions of the linear collisionless dispersion relation can be used to calculate the heat deposited into the ions and electrons for a given linear wave mode. These results for ion to electron power are verified against estimates of the heating from the hot plasma dispersion relation and compared to numerical results from GS2 (i.e., numerical calculation of the heating using equation (B9)) in Figure 5. Here we have plotted the ion to electron power for a temperature ratio of $T_{0i}/T_{0e} = 100$ and ion plasma beta values of $\beta_i = 1, 10$. The GS2 results agree well with the linear gyrokinetic and linear hot plasma calculations over five orders of magnitude in the power ratio.

3.3. Density Fluctuations

Alfvén waves in the MHD limit (at large scales) are incompressible, with no motion along the magnetic field and no associated density fluctuation. But as Alfvén waves non-linearly cascade to small scales of order $k_{\perp}\rho_i \sim 1$, finite Larmor radius effects give rise to non-zero parallel motions, driving density fluctuations. Here we compare the density fluctuations predicted by the linear gyrokinetic dispersion relation with that from hot plasma theory. Figure 6 compares the density fluctuations for a plasma with temperature ratio $T_{0i}/T_{0e} = 1$ and values of ion plasma beta $\beta_i = 0.1$, 1, and 10, parameter values relevant to the observations of interstellar scintillation in the ISM. These results demonstrate that the fractional electron density fluctuations $|\delta n_{0e}|/n_{0e}$, normalized by the electron velocity fluctuation, peak near the ion Larmor radius as expected.

3.4. Collisions

Gyrokinetic theory is valid in both the collisionless and collisional limits. To demonstrate the effect of increasing collisionality—implemented in GS2 using a pitch-angle scattering operator on each species with a coefficient ν_s —Figure 7 presents the measured linear damping rate in GS2 as the collisionality is increased. Parameters for this demonstration are $\beta_i = 10$, $T_{0i}/T_{0e} = 100$, and $k_{\perp}\rho_i = 1.414$; the collision rates for both species are set to be equal,

 $\nu = \nu_{ii} = \nu_{ee}$, and interspecies collisions are turned off. The figure clearly demonstrates that in the collisionless limit, $\nu \ll \omega$, the damping rate due to collisionless processes becomes independent of ν . As the collision rate is increased, heating via collisionless Landau damping becomes less effective and the measured damping rate decreases; this is expected because, in the MHD limit where collisions dominate, Alfvén waves are undamped. As discussed in §2.4, however, all heating is ultimately collisional—collisions are necessary to smooth out the small-scale structure in velocity space produced by wave-particle interactions. A minimum collision rate must be specified for the determination of the heating rate to converge. In the low velocity-space resolution runs (10 × 8 in velocity space) presented in Figure 7, for $\nu/(k_{\parallel}v_A) < 0.01$, the heating rate did not converge accurately. Increasing the velocity-space resolution lowers the minimum threshold on the collision rate necessary to achieve convergence, but some minimum collision rate is always necessary to realize a resolved algorithm by smoothing out the small-scale structure in velocity space.

3.5. Limits of Applicability

The gyrokinetic theory derived here is valid as long as three important conditions are satisfied: (1) $k_{\parallel} \ll k_{\perp}$, (2) $\omega \ll \Omega_i$, and (3) $v_{th_s} \ll c$ (again, the nonrelativistic assumption is not essential, but it is assumed in our derivation).

A demonstration of the breakdown of the gyrokinetic approximation when these limits are exceeded is provided in Figure 8 for a plasma with $T_{0i}/T_{0e}=1$, $\beta_i=1$, and $k_{\perp}\rho_i=0.1$. Here, we increase the ratio of the parallel to perpendicular wavenumber k_{\parallel}/k_{\perp} from 0.001 to 100, and solve for the frequency using the hot plasma dispersion relation; the frequency increases towards the ion cyclotron frequency as the wavenumber ratio approaches unity. The normalized frequency $\omega/(k_{\parallel}v_A)$ in gyrokinetics is independent of the value of k_{\parallel} , so we compare these gyrokinetic values with the hot plasma solution. Figure 8 plots the normalized real frequency $\omega/(k_{\parallel}v_A)$ and damping rate $|\gamma|/(k_{\parallel}v_A)$ against the ratio of the real frequency to the ion cyclotron frequency ω/Ω_i . Also plotted is the value of k_{\parallel}/k_{\perp} at each ω/Ω_i . At $\omega/\Omega_i \sim 0.01$ (and $k_{\parallel}/k_{\perp} \sim 0.1$), the damping rate deviates from the gyrokinetic solution as cyclotron damping begins to become important; the real frequency departs from the gyrokinetic results at $\omega/\Omega_i \sim 0.1$ (and $k_{\parallel}/k_{\perp} \sim 1$). It is evident that gyrokinetic theory gives remarkably good results even when $k_{\parallel}/k_{\perp} \sim 0.1$.

4. Discussion

This paper is the first in a series to study the properties of low frequency anisotropic turbulence in collisionless plasmas using gyrokinetics. Our primary motivation for investigating this problem is that such turbulence appears to be a natural outcome of MHD turbulence as energy cascades to small scales nearly perpendicular to the direction of the local magnetic field, as in Figure 1. Gyrokinetic turbulence may thus be a generic feature of turbulent astrophysical plasmas.

Gyrokinetics is an approximation to the full theory of collisionless and collisional plasmas. The necessary assumptions are that turbulent fluctuations are anisotropic with parallel wavenumbers small compared to perpendicular wavenumbers, $k_{\parallel} \ll k_{\perp}$, that frequencies are small compared to the ion cyclotron frequency, $\omega \ll \Omega_i$, and that fluctuations are small so that the typical plasma or field line displacement is of order $\mathcal{O}(k_{\perp}^{-1})$. In this limit, one can average over the Larmor motion of particles, simplifying the dynamics considerably. Although gyrokinetics assumes $\omega \ll \Omega_i$, it allows for $k_{\perp}\rho_i \sim 1-i.e.$, wavelengths in the direction perpendicular to the magnetic field can be comparable to the ion Larmor radius. On scales $k_{\perp}\rho_i \lesssim 1$, the gyrokinetic approximation orders out the fast MHD wave, but retains the slow wave and the Alfvén wave. Gyrokinetics also orders out cyclotron frequency effects such as cyclotron resonant heating, but retains collisionless damping via the Landau resonance. It is also worth noting that reconnection in the presence of a strong guide field can be described by gyrokinetics; thus current sheets that develop on scales of less than or equal to ρ_i in a turbulent plasma are self-consistently modeled in a nonlinear gyrokinetic simulation. The enormous value of gyrokinetics as an approximation is threefold: first, it considerably simplifies the linear and nonlinear equations; second, it removes the fast cyclotron time-scales and the gyro-angle dimension of phase space; and third, it allows for a simple physical interpretation in terms of the motion of charged rings.

In this paper, we have presented a derivation of the gyrokinetic equations, including for the first time the equations describing particle heating and global energy conservation. The dispersion relation for linear collisionless gyrokinetics is derived and its physical interpretation is discussed: on scales $k_{\perp}\rho_i \sim 1$, there is a linear mixing of the Alfvén and slow waves. This leads to effects such as collisionless damping of the Alfvén wave and finite density fluctuations in linear Alfvén waves. We have compared the gyrokinetic results with those of hot plasma kinetic theory, showing the robustness of the gyrokinetic approximation. We also used comparisons with the analytical results from both theories to verify and demonstrate the accuracy of the gyrokinetic simulation code GS2 in the parameter regimes of astrophysical interest. We note that although our tests are linear, GS2 has been used extensively for nonlinear turbulence problems in the fusion research (e.g., Dorland et al. 2000; Jenko et al.

2000; Rogers et al. 2000; Jenko et al. 2001; Jenko and Dorland 2001, 2002; Candy et al. 2004; Ernst et al. 2004).

To conclude, we briefly describe several of the astrophysics problems that will be explored in more detail in future work:

- 1. Energy in Alfvénic turbulence is weakly damped until it cascades to $k_{\perp}\rho_i \sim 1$. Thus gyrokinetics can be used to calculate the species by species heating of plasmas by MHD turbulence. In future work we will carry out such calculations and apply them to particle heating in solar flares, the solar wind, and hot radiatively inefficient accretion flows Quataert (see 1998); Gruzinov (see 1998); Quataert and Gruzinov (see 1999); Leamon et al. (see 1998, 1999, 2000); Cranmer and van Ballegooijen (see 2003, 2005, for related analytical work.).
- 2. In situ observations of the turbulent solar wind directly measure the magnetic field (Goldstein et al. 1995; Leamon et al. 1998, 1999), electric field (Bale et al. 2005), and density power spectra down to scales smaller than the ion gyroradius. Thus detailed quantitative comparisons between simulated power spectra and the measured ones are possible. It is worth noting, however, that the solar wind is in fact sufficiently collisionless that the gyrokinetic ordering here is not appropriate and that the equilibrium distribution function F_0 may deviate from a Maxwellian. But significant distortions of F_0 are tempered by high-frequency kinetic instabilities that may play the role of collisions in smoothing out the distribution function, so the solar wind plasma may not depart significantly from gyrokinetic behavior.
- 3. In the interstellar medium of the Milky Way, Armstrong et al. (1995) have inferred a density fluctuation power spectrum that is consistent, over 10 decades in spatial scale, with Kolmogorov turbulence. Observations suggest the existence of an inner scale to the density fluctuations at approximately the ion Larmor radius (Spangler and Gwinn 1990). These observations may be probing the density fluctuations associated with Alfvén waves on gyrokinetic scales (see §3.3 and Figure 6)—precisely the regime that is best investigated by gyrokinetic simulations.

Much of this work was supported by the DOE Center for Multi-scale Plasma Dynamics, Fusion Science Center Cooperative Agreement ER54785. E. Q. is also supported in part by NSF grant AST 0206006, NASA grant NAG5-12043, an Alfred P. Sloan Fellowship, and the David and Lucile Packard Foundation. A. A. S. was supported by the UKAFF Fellowship, and subsequently by the PPARC Advanced Fellowship and by King's College, Cambridge.

REFERENCES

- Abramowitz, M. and Stegun, I. A. 1972, Handbook of Mathematical Functions, 9th. ed., New York: Dover.
- Antonsen, T. M. and Lane, B. 1980, Phys. Fluids, 23, 1205.
- Armstrong, J. W., Rickett, B. J., and Spangler, S. R. 1995, ApJ, 443, 209.
- Bale, S. D., Kellogg, P. J., Mozer, F. S., Horbury, T. S., and Reme, H. 2005, arXiv:physics/0503103.
- Barnes, A. 1966, Phys. Fluids, 9, 1483.
- Beer, M. A., Cowley, S. C., and Hammett, G. W. 1995, Phys. Plasmas, 2, 2687.
- Belcher, J. W. and Davis, L. 1971, J. Geophys. Res., 76, 3534
- Candy, J., Waltz, R. E. and Dorland, W. 2004, Phys. Plasmas, 11, L25.
- Catto, P. J. 1978, Plasma Phys., 20, 719.
- Catto, P. J., Tang, W. M., and Baldwin, D. E., 1981, Plasma Phys., 23, 639.
- Cho, J., Lazarian, A., and Vishniac, E. T. 2002, ApJ, 564, 291.
- Cranmer, S. R. and van Ballegooijen, A. A. 2003, ApJ, 594, 573.
- Cranmer, S. R. and van Ballegooijen, A. A. 2005, ApJS, 156, 265.
- Dorland, W., Jenko, F., Kotschenreuther, M. and Rogers, B. N. 2000, Phys. Rev. Lett., 85, 5579.
- Dorland, W. D., Cowley, S. C., Hammett, G. W., Howes, G. G., Quataert, E., and Schekochihin, A. A. 2006, Phys. Plasmas, to be published.
- Dubin, D. H. E., Krommes, J. A., Oberman, C., and Lee, W. W. 1983, Phys. Fluids, 26, 3524.
- Ernst, D. R., Bonoli, P. T., Catto, P. J., Dorland, W., Fiore, C. L., Graentz, R. S., Greenwald, M., Hubbard, A. E., Porkolab, M., Redi, M. H., Rice, J. E., Zhurovich, K., and the Alcator C-Mod Group, 2004, Phys. Plasmas, 11, 2637.
- Foote, E. A. and Kulsrud, R. M. 1979, ApJ, 233, 302.

Fried, B. D. and Conte, S. D. 1961, The Plasma Dispersion Function, New York: Academic Press.

Frieman, E. A. and Chen, L. 1982, Phys. Fluids, 25, 502.

Goldreich, P. and Sridhar, S. 1995, ApJ, 438, 763.

Goldreich, P. and Sridhar, S. 1995, ApJ, 485, 688.

Goldstein, M. L., Roberts, D. A., and Matthaeus, W. H. 1995, ARA&A, 33, 283.

Gruzinov, A. 1998, ApJ, 501, 787.

Hahm, T. S., Lee, W. W., and Brizard, A. 1988, Phys. Fluids, 31, 1940.

Hasegawa, A. and Chen, L. 1975, Phys. Rev. Lett., 35, 370.

Higdon, J. C. 1984, ApJ, 285, 109.

Higdon, J. C. 1986, ApJ, 309, 342.

Huba, J. D., ed. 2004, NRL Plasma Formulary, NRL/PU/6790-04-477, (Washington: Naval Research Laboratory).

Jenko, F., Dorland, W., Kotschenreuther, M. and Rogers, B. N. 2000, Phys. Plasmas, 7, 1094.

Jenko, F. and Dorland, W. 2001, Plasma Phys. Control. Fusion, 43, A141.

Jenko, F. and Dorland, W. 2002, Phys. Rev. Lett., 89, 225001-1.

Jenko, F., Dorland, W., and Hammett, G. W. 2001, Phys. Plasmas, 8, 4096.

Kingsep, A. S., Chukbar, K. V., and Yankov, V. V. 1990, Rev. Plasma Phys., 16, 24.

Kolmogorov, A. N. 1941, Dokl. Akad. Nauk SSSR, 30, 9.

Kotschenreuther, M., Rewoldt, G., and Tang, W. M. 1995, Comp. Phys. Comm., 88, 128.

Krall, N. A. and Trivelpiece, A. W. 1986, Principles of Plasma Physics, San Francisco: San Francisco Press.

Krommes, J. A. and Hu, G. 1994, Phys. Plasmas, 1, 3211.

Leamon, R. J., Smith, C.W., Ness, N. F., Matthaeus, W. H., and Wong, H. K. 1998, J. Geophys. Res., 103, 4775. Leamon, R. J., Smith, C.W., Ness, N. F., and Wong, H. K. 1999, J. Geophys. Res., 104, 22331.

Leamon, R. J., Matthaeus, W. H., Smith, C.W., Zank, G. P., Mullan, D. J., and Oughton, S. 2000, ApJ, 537, 1054.

Lifshitz, E. M. and Pitaevskii, L. P. 1981, Physical Kinetics, New York: Pergamon Press. American Institute of Physics.

Lithwick, Y. and Goldreich, P. 2001, ApJ, 562, 279.

Lithwick, Y. and Goldreich, P. 2003, ApJ, 582, 1220.

Maron, J. and Goldreich, P. 2001, ApJ, 554, 1175.

Matthaeus, W. H., Goldstein, M. L., and Roberts, D. A. 1990, J. Geophys. Res., 95, 20673

Mongomery, D and Turner, L. 1981, Phys. Fluids, 24 825.

Quataert, E. 1998, ApJ, 500, 978.

Quataert, E. and Gruzinov, A. 1999, ApJ, 520, 248.

Rogers, B. N., Dorland, W., and Kotschenreuther, M. 2000, Phys. Rev. Lett., 85, 5336.

Rutherford, P. H. and Frieman, E. A. 1968, Phys. Fluids, 11, 569.

Schekochihin, A. A. and Cowley, S. C. 2005, in Magnetohydrodynamics: Historical Evolution and Trends, ed. S. Molokov, R. Moreau, & H. K. Moffatt, (Berlin: Springer), to be published (e-print astro-ph/0507686).

Schekochihin, A. A. and Cowley, S. C. 2006, Phys. Plasmas, to be published.

Schekochihin, A. A., Cowley, S. C., Dorland, W. D., Hammett, G. W., Howes, G. G., and Quataert, E. 2006, ApJ, to be published.

Shakura, N. I. and Sunyaev, R. A. 1973, A&A, 24, 337.

Shebalin, J. V., Matthaeus, W. H., and Montgomery, D. 1983, J. Plasma Phys., 29, 525.

Spangler, S. R. and Gwinn, C. R. 1990, ApJ, 353, 29.

Sridhar, S. and Goldreich, P. 1994, ApJ, 432, 612.

Stix, T. H. 1992, Waves in Plasmas, New York: American Institute of Physics.

Taylor, J. B. and Hastie, R. J. 1968, Phys. Fluids, 10, 479.

Watson, G. N. 1966, A Treatise on the Theory of Bessel Functions, 2nd. ed., (Cambridge: Cambridge University Press).

Wilkinson, P. N., Narayan, R., and Spencer, R. E. 1994, MNRAS, 269 67.

A. Derivation of the Gyrokinetic Equations

In this appendix, we derive the nonlinear gyrokinetic equation in the simple case where the equilibrium is a homogeneous plasma in a constant magnetic field, i.e., $\nabla F_0 = 0$ and $\mathbf{B}_0 = B_0 \hat{\mathbf{z}}$ in a periodic box. The nonlinear gyrokinetic equation in an inhomogeneous plasma was first derived by Frieman and Chen (1982). Here, we proceed one more order in the expansion, to the transport order, and calculate the heating rate (for the first time). We begin with the Fokker-Planck equation and Maxwell's equations. The basic ordering, the most suitable coordinates, and the necessary ring averages are defined in §2. The Fokker-Planck equation is expanded under the gyrokinetic ordering as described in §2.1. The minus first, zeroth and first orders are solved to determine both the form of the equilibrium distribution function and the evolution equation for the perturbed distribution function—the gyrokinetic equation. At each order, a ring average at constant guiding center position is employed to eliminate higher orders from the equation. Velocity integration of the perturbed distribution function yields the charge and current densities that appear in the gyrokinetic counterparts of Maxwell's equations.

A.1. Maxwell's Equations—Potentials

Applying the gyrokinetic ordering, as described in detail in §2.1, to Faraday's Law demonstrates that to lowest order $\nabla \times \delta \mathbf{E} = 0$, so the electric field is dominantly electrostatic. The inductive electric field, however, gives an important contribution to the parallel electric field. This motivates the introduction of the scalar potential ϕ and vector potential \mathbf{A} for the electric and magnetic field,

$$\delta \mathbf{E} = -\nabla \phi - \frac{1}{c} \frac{\partial \mathbf{A}}{\partial t} \tag{A1}$$

This preprint was prepared with the AAS IATEX macros v5.2.

and

$$\delta \mathbf{B} = \nabla \times \mathbf{A}.\tag{A2}$$

We choose the Coulomb gauge $\nabla \cdot \mathbf{A} = 0$. Thus with the gyrokinetic ordering, to $\mathcal{O}(\epsilon^2)$, the vector potential is

$$\mathbf{A} = A_{\parallel} \hat{\mathbf{z}} + \mathbf{A}_{\perp} = A_{\parallel} \hat{\mathbf{z}} + \nabla \lambda \times \hat{\mathbf{z}}. \tag{A3}$$

Hence, the perturbed magnetic field to $\mathcal{O}(\epsilon^2)$ is given by

$$\delta \mathbf{B} = \nabla A_{\parallel} \times \hat{\mathbf{z}} - \nabla^2 \lambda \hat{\mathbf{z}} = \nabla A_{\parallel} \times \hat{\mathbf{z}} + \delta B_{\parallel} \hat{\mathbf{z}}. \tag{A4}$$

We will use the scalars A_{\parallel} and δB_{\parallel} (rather than λ) in subsequent development. Under the gyrokinetic ordering the displacement current may be dropped, leaving Ampère's Law

$$\nabla \times \delta \mathbf{B} = -\nabla^2 \mathbf{A} = -\nabla^2 A_{\parallel} \hat{\mathbf{z}} + \nabla \delta B_{\parallel} \times \hat{\mathbf{z}} = \frac{4\pi}{c} \delta \mathbf{J}. \tag{A5}$$

Finally, the ordering in Coulomb's Law requires that $\nabla \cdot \delta \mathbf{E}$ is much smaller than $4\pi \sum_{s} q_{s} n_{0s}$, yielding the quasineutrality condition

$$\sum_{s} q_s n_{0s} = 0. \tag{A6}$$

A.2. The Gyrokinetic Equation

To reduce the clutter, we suppress the species label s in this section. The derivation of the gyrokinetic equation is clarified by the use of transformed coordinates for position and velocity. The guiding center position is defined by: $\mathbf{R} = \mathbf{r} - (\hat{\mathbf{z}} \times \mathbf{v})/\Omega$ (see §2.2). The velocity coordinates are usefully expressed in terms of the total velocity v, perpendicular velocity v_{\perp} , and gyrophase angle θ , defined by

$$v = \sqrt{v_x^2 + v_y^2 + v_z^2}, \quad v_{\perp} = \sqrt{v_x^2 + v_y^2}, \quad \theta = \tan^{-1}\left(\frac{v_y}{v_x}\right).$$
 (A7)

(Note that in the inhomogeneous case, it is more convenient to use the energy $E = mv^2/2$ and the first adiabatic invariant (the magnetic moment) $\mu = (1/2)mv_{\perp}^2/B$ instead of v and v_{\perp} .)

The orderings are motivated and developed in §2.1. Here we summarize the ordering for easy reference:

$$\frac{\delta f}{F_0} \sim \frac{|\delta \mathbf{B}|}{B_0} \sim \frac{c|\delta \mathbf{E}_{\perp}|}{v_{th}B_0} \sim \frac{\delta E_{\parallel}}{|\delta \mathbf{E}_{\perp}|} \sim \mathcal{O}(\epsilon),$$

$$\nabla_{\perp} \delta f \sim \mathcal{O}(\frac{\delta f}{\rho_i}) \quad \text{and} \quad \hat{\mathbf{z}} \cdot \nabla \delta f \sim \mathcal{O}(\frac{\delta f}{l_0}),$$

$$\frac{1}{\delta \mathbf{B}} \frac{\partial \delta \mathbf{B}}{\partial t} \sim \frac{1}{\delta \mathbf{E}} \frac{\partial \delta \mathbf{E}}{\partial t} \sim \frac{1}{\delta f} \frac{\partial \delta f}{\partial t} \sim \mathcal{O}(\frac{v_{th}}{l_0}) \quad \text{and} \quad \frac{1}{F_0} \frac{\partial F_0}{\partial t} \sim \mathcal{O}(\frac{\epsilon^2 v_{th}}{l_0}).$$
(A8)

With this ordering, the order of every term in the Fokker-Planck equation becomes

$$\frac{\partial F_0/\partial t}{\epsilon^2} + \frac{\partial \delta f/\partial t}{\epsilon} + \mathbf{v}_{\perp} \cdot \nabla \delta f + v_{\parallel} \hat{\mathbf{z}} \cdot \nabla \delta f \\
+ \frac{q}{mc} (-c\nabla \phi - \partial \mathbf{A}/\partial t + \mathbf{v} \times \delta \mathbf{B} + \mathbf{v} \times \mathbf{B}_0) \cdot \partial F_0/\partial \mathbf{v} \\
1 & \epsilon & 1 & 1/\epsilon \\
+ \frac{q}{mc} (-c\nabla \phi - \partial \mathbf{A}/\partial t + \mathbf{v} \times \delta \mathbf{B} + \mathbf{v} \times \mathbf{B}_0) \cdot \partial \delta f/\partial \mathbf{v} \\
\epsilon & \epsilon^2 & \epsilon & 1 \\
= C(F_0, F_0) + C(\delta f, F_0) + C(F_0, \delta f) & + C(\delta f, \delta f), \\
1 & \epsilon & \epsilon^2 & \epsilon^2$$
(A9)

where we label below each term its order relative to $F_0v_{th_i}/l_0$ in powers if ϵ . C(f,f) is the standard Fokker-Planck integro-differential collision operator (e.g., Huba 2004). We denote the power of ϵ in the expansion of the perturbation to the distribution function by a subscript $\delta f = \delta f_1 + \delta f_2 + \cdots$ and $\delta f_i \sim \mathcal{O}(\epsilon^i F_0)$. We now proceed with the formal expansion.

Minus First Order, $\mathcal{O}(1/\epsilon)$:. From equation (A9), in velocity variables transformed from \mathbf{v} to (v, v_{\perp}, θ) , we obtain at this order

$$\frac{\partial F_0}{\partial \theta} = 0,\tag{A10}$$

so the equilibrium distribution function does not depend on gyrophase angle, $F_0 = F_0(v, v_{\perp}, t)$.

Zeroth order, $\mathcal{O}(1)$:. At this order, equation (A9) becomes

$$\mathbf{v}_{\perp} \cdot \nabla \delta f_1 + \frac{q}{mc} \{ -c \nabla \phi + \mathbf{v} \times \delta \mathbf{B} \} \cdot \frac{\partial F_0}{\partial \mathbf{v}} - \Omega \frac{\partial \delta f_1}{\partial \theta} = C(F_0, F_0). \tag{A11}$$

At this stage both F_0 and δf_1 are unknown. To eliminate δf_1 from this equation (and thereby isolate information about F_0), we multiply equation (A11) by $1 + \ln F_0$ and integrate over all space and velocity space, making use of the periodic boundary conditions for perturbed quantities and equation (A10), to find

$$\int d^3 \mathbf{r} d^3 \mathbf{v} (\ln F_0) C(F_0, F_0) = 0.$$
 (A12)

It is known from the proof of Boltzmann's H Theorem (see §B.2) that this implies that F_0 is a Maxwellian, *i.e.*,

$$F_0 = \frac{n_0}{\pi^{3/2}} \frac{1}{v_{th}^3} \exp\left(-\frac{v^2}{v_{th}^2},\right) \tag{A13}$$

where the mean plasma flow is assumed to be zero. The temperature $T_0(t) = (1/2)mv_{th}^2$ of this Maxwellian varies on the long heating time-scale, $t_{heat} \sim \mathcal{O}(\epsilon^{-2}L/v_{th})$, due to turbulent

heating. We determine this heating in second order—see §B. The density n_0 does not vary since the number of particles is conserved. In all other derivations of gyrokinetics, F_0 is not determined, although it is often assumed to be a Maxwellian.

Substituting the solution for F_0 (equation (A13)) into equation (A11) (and using $C(F_0, F_0) = 0$) yields

$$\mathbf{v}_{\perp} \cdot \nabla \delta f_1 - \Omega \frac{\partial \delta f_1}{\partial \theta} = -\mathbf{v} \cdot \nabla \left(\frac{q\phi}{T_0} \right) F_0. \tag{A14}$$

This inhomogeneous equation for δf_1 supports a particular solution and a homogeneous solution. Noting the particular solution $\delta f_p = -\frac{q\phi}{T_0}F_0 + \mathcal{O}(\epsilon^2)$, our solution for the first-order perturbation is written as $\delta f_1 = -\frac{q\phi}{T_0}F_0 + h$. To $\mathcal{O}(\epsilon^2)$, the homogeneous solution h satisfies

$$\mathbf{v}_{\perp} \cdot \nabla h - \Omega \left(\frac{\partial h}{\partial \theta} \right)_{\mathbf{r}} = \left(\frac{\partial h}{\partial \theta} \right)_{\mathbf{R}} = 0,$$
 (A15)

where we have transformed the θ -derivative at constant position \mathbf{r} to one at constant guiding center \mathbf{R} . Thus h is independent of the gyrophase angle at constant guiding center \mathbf{R} (but not at constant position \mathbf{r})—i.e., $h = h(\mathbf{R}, v, v_{\perp}, t)$. Our complete solution for the distribution function at this order, after taking $1 - q\phi/T_0 = \exp(-q\phi/T_0) + \mathcal{O}(\epsilon^2)$ and absorbing several $\mathcal{O}(\epsilon^2)$ terms into δf_2 , is

$$f = F_0(v, \tau) \exp(-\frac{q\phi(\mathbf{r}, t)}{T_0}) + h(\mathbf{R}, v, v_\perp, t) + \delta f_2 + \cdots$$
(A16)

The first term in the solution is the equilibrium distribution function corrected by the Boltzmann factor. Physically this arises from the rapid (compared to the evolution of ϕ) motion of particles across the field lines attempting to set up a thermal equilibrium distribution. However the motion of the particles across the field is constrained by the gyration and the particles are not (entirely) free to set up thermal equilibrium. The second term is the gyrokinetic distribution function that represents the response of the rings to the perturbed fields.

First order, $\mathcal{O}(\epsilon)$:. Plugging in the form of solution given in equation (A16) and transforming into guiding-center spatial coordinates and velocity coordinates (v, v_{\perp}, θ) , the Fokker-Planck equation to this order becomes

$$\frac{\partial h}{\partial t} + \frac{d\mathbf{R}}{dt} \cdot \frac{\partial h}{\partial \mathbf{R}} + \frac{q}{mc} \{ -c\nabla\phi + \mathbf{v} \times \delta\mathbf{B} \} \cdot \left\{ \frac{\mathbf{v}}{v} \frac{\partial h}{\partial v} + \frac{\mathbf{v}_{\perp}}{v_{\perp}} \frac{\partial h}{\partial v_{\perp}} \right\} - \left(\frac{\partial h}{\partial t} \right)_{\text{coll}} =$$

$$\Omega \left(\frac{\partial \delta f_2}{\partial \theta} \right)_{\mathbf{R}} + \frac{q}{T_0} \left(\frac{\partial \phi}{\partial t} - \frac{\mathbf{v}}{c} \cdot \frac{\partial \mathbf{A}}{\partial t} \right) F_0, \quad (A17)$$

where $\left(\frac{\partial h}{\partial t}\right)_{\text{coll}} = C(h, F_0) + C(F_0, h)$ is the linearized collision operator (note that it involves h and F_0 both of electrons and of ions). To eliminate δf_2 from this equation, we ring average

the equation over θ at fixed guiding center **R**, taking advantage of the fact that δf_2 must be periodic in θ , to obtain

$$\frac{\partial h}{\partial t} + \left\langle \frac{d\mathbf{R}}{dt} \right\rangle_{\mathbf{R}} \cdot \frac{\partial h}{\partial \mathbf{R}} - \left\langle \left(\frac{\partial h}{\partial t} \right)_{\text{coll}} \right\rangle_{\mathbf{R}} = \frac{q}{T_0} \frac{\partial \langle \chi \rangle_{\mathbf{R}}}{\partial t} F_0, \tag{A18}$$

where we have defined the gyrokinetic potential

$$\chi = \phi - \frac{\mathbf{v} \cdot \mathbf{A}}{c}.\tag{A19}$$

After a straightforward calculation, we find that the ring averaged guiding center motion is given by

$$\left\langle \frac{d\mathbf{R}}{dt} \right\rangle_{\mathbf{R}} = v_{\parallel} \hat{\mathbf{z}} - \frac{c}{B_0} \frac{\partial \langle \chi \rangle_{\mathbf{R}}}{\partial \mathbf{R}} \times \hat{\mathbf{z}}. \tag{A20}$$

Substituting this result into equation (A19), we obtain the **gyrokinetic equation**:

$$\frac{\partial h}{\partial t} + v_{\parallel} \hat{\mathbf{z}} \cdot \frac{\partial h}{\partial \mathbf{R}} + \frac{c}{B_0} \left[\langle \chi \rangle_{\mathbf{R}}, h \right] - \left\langle \left(\frac{\partial h}{\partial t} \right)_{\text{coll}} \right\rangle_{\mathbf{R}} = \frac{q}{T_0} \frac{\partial \langle \chi \rangle_{\mathbf{R}}}{\partial t} F_0, \tag{A21}$$

where the nonlinear effects enter via the Poisson bracket, defined by

$$[\langle \chi \rangle_{\mathbf{R}}, h] = \left(\frac{\partial \langle \chi \rangle_{\mathbf{R}}}{\partial \mathbf{R}} \times \hat{\mathbf{z}}\right) \cdot \frac{\partial h}{\partial \mathbf{R}} = \frac{\partial \langle \chi \rangle_{\mathbf{R}}}{\partial x} \frac{\partial h}{\partial y} - \frac{\partial \langle \chi \rangle_{\mathbf{R}}}{\partial y} \frac{\partial h}{\partial x}.$$
 (A22)

The gyrokinetic equation (A21) describes the time evolution of h, the ring distribution function. The second term on the left-hand side corresponds to the ring motion along \mathbf{B}_0 , the third term the ring motion across \mathbf{B}_0 , the fourth term the effect of collisions. The source term on the right-hand side represents the ring-averaged change in the energy of the particles. A more detailed discussion of the physical aspects of this equation is given in §2.3. The equilibrium distribution function F_0 changes only on the transport time-scale and is thus formally fixed (stationary) with respect to the time-scale of this equation. The evolution of F_0 will be calculated in §B.1.

A.3. The Gyrokinetic Form of Maxwell's Equations

To complete the set of gyrokinetic equations, we need to determine Maxwell's equations to first order $\mathcal{O}(\epsilon)$ in the gyrokinetic ordering. The equations we use are Ampère's law equation (A5), the quasineutrality condition equation (A6), and the definitions of the scalar (equation (A1)) and vector (equations (A3) and (A4)) potentials.

A.3.1. The Quasineutrality Condition

The charge density needed in the quasineutrality condition, equation (A6), can by determined by multiplying the distribution function, equation (A16), expanded to first order $\mathcal{O}(\epsilon)$, by the charge q_s and integrating over velocity. Expanding the exponential in the Boltzmann term and dropping terms of order $\mathcal{O}(\epsilon^2)$ and higher gives

$$\sum_{s} \left(-\frac{q_s^2 n_{0s}}{T_{0s}} \phi + q_s \int d^3 \mathbf{v} h_s (\mathbf{r} + \frac{\mathbf{v} \times \hat{\mathbf{z}}}{\Omega_s}, \mathbf{v}, t) \right) = 0.$$
 (A23)

Note that the integral over gyrophase angle in the velocity must be performed at fixed position \mathbf{r} , because the charge must be determined at fixed position \mathbf{r} , not at fixed guiding center \mathbf{R} . Therefore, we perform a ring average at fixed position \mathbf{r} to produce the final form of the quasineutrality condition

$$\sum_{s} \left(-\frac{q_s^2 n_{0s}}{T_{0s}} \phi + q_s \int d^3 \mathbf{v} \langle h_s \rangle_{\mathbf{r}} \right) = 0.$$
 (A24)

A.3.2. The Parallel Ampère's Law

Here we take the parallel component of Ampère's Law, equation (A5), finding the current by multiplying the distribution function, equation (A16), expanded to first order $\mathcal{O}(\epsilon)$, by the charge times velocity $q_s \mathbf{v}$ and integrating over velocity. The Boltzmann part of the current is odd over v_{\parallel} and vanishes upon integration. Performing a ring average at fixed position \mathbf{r} yields the the parallel component of Ampère's Law

$$-\nabla_{\perp}^{2} A_{\parallel} = \frac{4\pi}{c} \delta J_{\parallel} = \sum_{s} \frac{4\pi}{c} q_{s} \int d^{3} \mathbf{v} v_{\parallel} \langle h_{s} \rangle_{\mathbf{r}}. \tag{A25}$$

A.3.3. The Perpendicular Ampère's Law

The perpendicular component of Ampère's Law, equation (A5), is derived in an analogous manner as the parallel component in §A.3.2: Ampère's Law is crossed with $\hat{\mathbf{z}}$, the Boltzmann contribution vanishes upon integration over gyrophase angle θ , and a ring average at fixed position \mathbf{r} is performed. The final result is

$$\nabla_{\perp} \delta B_{\parallel} = \frac{4\pi}{c} \hat{\mathbf{z}} \times \delta \mathbf{J} = \sum_{\hat{\mathbf{z}}} \frac{4\pi}{c} q_s \int d^3 \mathbf{v} \langle \hat{\mathbf{z}} \times \mathbf{v}_{\perp} h_s \rangle_{\mathbf{r}}.$$
 (A26)

It is straightforward to show that equation (A26) is the gyrokinetic version of perpendicular pressure balance (no fast magnetosonic waves). Integration by parts yields:

$$\nabla_{\perp} \frac{B_0 \delta B_{\parallel}}{4\pi} = -\nabla_{\perp} \cdot \delta \mathbf{P}_{\perp} \tag{A27}$$

where the perpendicular pressure tensor is,

$$\delta \mathbf{P}_{\perp} = \sum_{s} m_{s} \int d^{3} \mathbf{v} \langle (\mathbf{v}_{\perp} \mathbf{v}_{\perp}) h_{s} \rangle_{\mathbf{r}}. \tag{A28}$$

In order to drive steady-state (not decaying) turbulence, we introduce additional externally driven antenna current J_a to the right hand sides of equation (A25) and equation (A26).

B. Derivation of the Transport and Heating Rate

While the gyrokinetic equation (A21) determines the evolution of the perturbation to the distribution function on the medium time-scale, we must go to second order $\mathcal{O}(\epsilon^2)$ in the gyrokinetic ordering to obtain the slow evolution of the equilibrium distribution function F_0 . This appendix contains two derivations of the heating rate: the first is the more conventional, but longer, derivation; the second derivation employs entropy conservation and is, in some sense, more intuitive.

B.1. Conventional Derivation of the Transport and Heating Rate

We begin by defining a medium-time-scale average over a period Δt long compared to the fluctuation time-scale but short compared to the heating time-scale, $1/\omega \ll \Delta t \ll 1/(\omega \epsilon^2)$,

$$\overline{a}(t) = \frac{1}{\Delta t} \int_{t-\Delta t/2}^{t+\Delta t/2} a(t')dt'.$$
(B1)

During this average the equilibrium distribution function F_0 is held constant.

To determine the evolution of the equilibrium density and temperature of a species s on the transport time-scale, we consider the full (not ring averaged) Fokker-Planck equation,

$$\frac{df_s}{dt} = C_{sr}(f_s, f_r) + C_{ss}(f_s, f_s), \tag{B2}$$

where $C_{sr}(f_s, f_r)$ denotes the effect of collisions of species s on species r and $C_{ss}(f_s, f_s)$ denotes like particle collisions.

To demonstrate that particle conservation implies n_{0s} is a constant, we integrate equation (B2) over all space (the periodic box) and velocity, divide by volume V, and discard all terms of order $\mathcal{O}(\epsilon^3)$ and higher to produce the result

$$\int \frac{d^3 \mathbf{r}}{V} \int d^3 \mathbf{v} \frac{\partial f_s}{\partial t} = \frac{\partial n_{0s}}{\partial t} + \frac{\partial}{\partial t} \int \frac{d^3 \mathbf{r}}{V} \int d^3 \mathbf{v} \delta f_{2s} = 0.$$
 (B3)

Here we have used the conservation of particles by the collision operator, the fact that the first-order perturbations spatially average to zero, and an integration by parts over velocity coupled with periodic boundary conditions to simplify the result. Performing the medium-time-scale average of equation (B1) eliminates the δf_{2s} term, leaving

$$\frac{\partial n_{0s}}{\partial t} = 0. {(B4)}$$

Thus, for both species s, the density n_{0s} is constant over the long time-scale.

The heating rate, and therefore the evolution of the temperature T_{0s} , is calculated similarly by multiplying equation (B2) by $\frac{1}{2}m_sv^2$, integrating over all space and velocity, and dividing by the box volume V. Using the expansion of the distribution function, an integration by parts in velocity, and the periodic boundary conditions, we find that:

$$\frac{3}{2}n_{0s}\frac{dT_{0s}}{dt} + \frac{\partial}{\partial t}\int \frac{d^3\mathbf{r}}{V}\int d^3\mathbf{v}\frac{1}{2}m_s v^2 \delta f_{2s} = \int \frac{d^3\mathbf{r}}{V}\int d^3\mathbf{v}q_s \mathbf{E} \cdot \mathbf{v}\int \frac{d^3\mathbf{r}}{V}\int d^3\mathbf{v}\frac{1}{2}m_s v^2 C_{sr}(f_s, f_r). \tag{B5}$$

The first term on the right-hand side is the work done on the particles by the fields, the second is the collisional energy exchange between species. Note that collisions between like particles do not produce a net loss of energy for a species and thus do not appear in this expression. At this order, the collisions between species occur only between the Maxwellian equilibria of each interacting species; the standard form of the collisional energy exchange (Huba 2004) is given by

$$\int \frac{d^3 \mathbf{r}}{V} \int d^3 \mathbf{v} \frac{1}{2} m_s v^2 C_{sr}(f_s, f_r) = n_{0s} \nu_E^{sr} (T_{0r} - T_{0s}).$$
 (B6)

A useful expression for the numerical value of this term is given in Huba (2004). The collisional energy exchange rate of ions on electrons is a factor $(m_e/m_i)^{1/2}$ times smaller than the ion-ion collision rate. It is therefore possible to sustain a temperature difference between ions and electrons even though the plasma is collisional enough to make F_0 Maxwellian for each species.

Splitting the electric field into its potentials $\mathbf{E} = -\nabla \phi - \frac{1}{c} \frac{\partial \mathbf{A}}{\partial t}$, we can manipulate the scalar potential part into a more useful higher order form. After some algebra and using

equation (B6), we find

$$\frac{3}{2}n_{0s}\frac{dT_{0s}}{dt} + \frac{d}{dt}\int \frac{d^{3}\mathbf{r}}{V}\int d^{3}\mathbf{v}\left(\frac{1}{2}m_{s}v^{2}\delta f_{2s} + q_{s}\phi\delta f_{s}\right)$$

$$= \int \frac{d^{3}\mathbf{r}}{V}\int d^{3}\mathbf{v}q_{s}\frac{\partial}{\partial t}\left(\phi - \frac{\mathbf{v}\cdot\mathbf{A}}{c}\right)\delta f_{s} + n_{0s}\nu_{E}^{sr}(T_{0r} - T_{0s}). \tag{B7}$$

From this equation, we can check the order of the heating rate,

$$\frac{3}{2}n_{0s}\frac{dT_{0s}}{dt} = \mathcal{O}(\epsilon^2 \omega T_{0s}); \tag{B8}$$

we see that the variation in the equilibrium quantities is, as expected, on a time scale that is ϵ^2 slower than the time scale of the variations in the fluctuating quantities. Note that this ordering is consistent with all the energy in an Alfvén wave cascade becoming heat in a single cascade time at the driving scale.

Splitting off the Boltzmann part of the perturbed distribution function, we obtain

$$\frac{3}{2}n_{0s}\frac{dT_{0s}}{dt} + \frac{d}{dt}\left[\int \frac{d^{3}\mathbf{r}}{V}\int d^{3}\mathbf{v}\left(\frac{1}{2}m_{s}v^{2}\delta f_{2s} + q_{s}\phi h_{s}\right) - \int \frac{d^{3}\mathbf{r}}{V}\frac{n_{0s}q_{s}^{2}\phi^{2}}{2T_{0s}}\right]$$

$$= \int \frac{d^{3}\mathbf{r}}{V}\int d^{3}\mathbf{v}q_{s}\frac{\partial\chi}{\partial t}h_{s} + n_{0s}\nu_{E}^{sr}(T_{0r} - T_{0s}). \tag{B9}$$

The medium-time-scale average, described by equation (B1), of the second term on left-hand side is zero; it does not contribute to the average heating. The first term on the right-hand side is the desired heating term that connects with the gyrokinetic equation.

To make this connection, we multiply the gyrokinetic equation (A21) by $T_{0s}h_s/F_{0s}$ and integrate over space and velocity to obtain

$$\frac{\partial}{\partial t} \int \frac{d^3 \mathbf{r}}{V} \int d^3 \mathbf{v} \frac{T_{0s}}{2F_{0s}} h_s^2 - \int \frac{d^3 \mathbf{r}}{V} \int d^3 \mathbf{v} \frac{T_{0s}}{F_{0s}} \left\langle h_s \left(\frac{\partial h_s}{\partial t} \right)_{\text{coll}} \right\rangle_{\mathbf{R}_s} = \int \frac{d^3 \mathbf{R}_s}{V} \int d^3 \mathbf{v} q_s \frac{\partial \langle \chi \rangle_{\mathbf{R}_s}}{\partial t} h_s. \tag{B10}$$

The heating term and the right-hand side of equation (B10) are in fact identical, *i.e.*, we can show by interchanging \mathbf{r} and \mathbf{v} integrations that

$$\int \frac{d^3 \mathbf{r}}{V} \int d^3 \mathbf{v} q_s \frac{\partial \chi}{\partial t} h_s = \int \frac{d^3 \mathbf{R}_s}{V} \int d^3 \mathbf{v} q_s \frac{\partial \langle \chi \rangle_{\mathbf{R}_s}}{\partial t} h_s, \tag{B11}$$

where the velocity integration on the right-hand side is done at fixed \mathbf{R}_s . Combining equations (B9) and (B10) using equation (B11) then gives an expression for the instantaneous heating

$$\frac{3}{2}n_{0s}\frac{dT_{0s}}{dt} + \frac{d}{dt}\left[\int \frac{d^{3}\mathbf{r}}{V}\int d^{3}\mathbf{v}\left(\frac{1}{2}m_{s}v^{2}\delta f_{2s} + q_{s}\phi h_{s} - \frac{T_{0s}}{2F_{0s}}h_{s}^{2}\right) - \int \frac{d^{3}\mathbf{r}}{V}\frac{n_{0s}q_{s}^{2}\phi^{2}}{2T_{0s}}\right]$$

$$= -\int \frac{d^{3}\mathbf{r}}{V}\int d^{3}\mathbf{v}\frac{T_{0s}}{F_{0s}}\left\langle h_{s}\left(\frac{\partial h_{s}}{\partial t}\right)_{coll}\right\rangle_{\mathbf{R}} + n_{0s}\nu_{E}^{sr}(T_{0r} - T_{0s}). \tag{B12}$$

The second term on the left-hand side of equation (B12) represents the sloshing of energy between particles and fields; this term averages to zero over the medium-time-scale average and thus does not contribute to the long-time-scale heating. On the right-hand side, the collisional term is negative definite for like particle and pitch-angle collision operators (these are the only relevant cases: for s = i, the ion-ion collisions dominate; for s = e, the dominant terms are electron-electron collisions and the pitch-angle scattering of the electrons off the ions; all other parts of the collision operator are subdominant by at least one factor of $(m_e/m_i)^{1/2}$). When equation (B12) is averaged over the medium-time-scale, this term yields the long-time-scale heating of species s

$$\frac{3}{2}n_{0s}\frac{dT_{0s}}{dt} = -\int \frac{d^3\mathbf{r}}{V} \int d^3\mathbf{v} \frac{T_{0s}}{F_{0s}} \overline{\left\langle h_s \left(\frac{\partial h_s}{\partial t} \right)_{\text{coll}} \right\rangle_{\mathbf{R}_s}} + n_{0s}\nu_E^{sr} (T_{0r} - T_{0s}). \tag{B13}$$

This expression for the long-time-scale heating is in some sense easier to average numerically than the instantaneous heating form of equation (B9) since it is sign-definite: unlike in equation (B9), calculating the average heating does not require precisely capturing the effect of near-cancellation of the medium-time-scale oscillations of the instantaneous energy transfer between particles and waves. It is also clear that the heating is collisional—when collisions are small, h_s will develop small scales in velocity space, typically $\Delta \mathbf{v} \sim \mathcal{O}(\nu^{1/2})$, so that the heating is essentially independent of the collision rate ν . As we see below, equation (B13) essentially relates heating to the collisional entropy production. It is essential for any kinetic code, such as GS2, to have some collisions to smooth the velocity distributions at small scales and resolve the entropy production.

B.2. Entropy Argument to Derive the Heating Rate

Ignoring the electron-ion collisions, which have a rate $(m_e/m_i)^{1/2}$ times smaller than the ion-ion collision rate, the Boltzmann H theorem for rate of change of entropy of the ions S_i is

$$\frac{dS_i}{dt} = -\frac{d}{dt} \int \frac{d^3 \mathbf{r}}{V} \int d^3 \mathbf{v} f_i \ln f_i = -\int \frac{d^3 \mathbf{r}}{V} \int d^3 \mathbf{v} \ln f_i C_{ii}(f_i, f_i). \tag{B14}$$

It can be easily shown that the right-hand side is greater than or equal to zero (Lifshitz and Pitaevskii 1981) and therefore that entropy always increases. It can also be shown that the entropy increase is zero if, and only if, the distribution function is a Maxwellian. Expanding the entropy about the Maxwellian equilibrium, we obtain, to second order $\mathcal{O}(\epsilon^2)$,

$$\frac{dS_i}{dt} = -\frac{d}{dt} \int \frac{d^3 \mathbf{r}}{V} \int d^3 \mathbf{v} \left[F_{0i} \ln F_{0i} + (1 + \ln F_{0i}) \delta f_{2i} + \frac{(\delta f_{1i})^2}{2F_{0i}} \right] = -\int \frac{d^3 \mathbf{r}}{V} \int d^3 \mathbf{v} \frac{\delta f_{1i}}{F_{0i}} \left(\frac{\partial \delta f_{1i}}{\partial t} \right)_{\text{coll}} (B15)$$

where we have made use of the energy conservation properties of ion-ion collisions and the fact that δf_{1i} has zero average over all space. Using the conservation of particles, the Maxwellian zeroth-order distribution function, and the definition of h_i , we obtain the slow evolution of temperature

$$\frac{3}{2}n_{0i}\frac{1}{T_{0i}}\frac{dT_{0i}}{dt} + \frac{d}{dt}\left[\int \frac{d^{3}\mathbf{r}}{V}\int d^{3}\mathbf{v}\left(\frac{1}{2}\frac{m_{i}v^{2}}{T_{0i}}\delta f_{2i} + \frac{q_{i}\phi h_{i}}{T_{0i}} - \frac{1}{2F_{0i}}h_{i}^{2}\right) - \int \frac{d^{3}\mathbf{r}}{V}\frac{n_{0i}q_{i}^{2}\phi^{2}}{2T_{0i}^{2}}\right]$$

$$= -\int \frac{d^{3}\mathbf{R}_{i}}{V}\int d^{3}\mathbf{v}\frac{1}{F_{0i}}\left\langle h_{i}\left(\frac{\partial h_{i}}{\partial t}\right)_{\text{coll}}\right\rangle_{\mathbf{R}_{i}}.$$
(B16)

This result is the same as equation (B12); the heating is clearly seen as irreversible entropy production. Over a medium-time-scale average, the second term on the left-hand side of equation (B16) vanishes, leaving a net heating that is the medium-time-scale average of the entropy production term on the right-hand side of equation (B16)—the same as the heating term on the right-hand side of equation (B13).

B.3. Energy Conservation in Driven Systems

To determine an equation for the conservation of energy in gyrokinetics, we use Poynting's Theorem

$$\frac{d}{dt} \int d^3 \mathbf{r} \left(\frac{E^2}{8\pi} + \frac{B^2}{8\pi} \right) + \frac{c}{4\pi} \oint (\mathbf{E} \times \mathbf{B}) \cdot d\mathbf{S} = -\int d^3 \mathbf{r} (\mathbf{J} + \mathbf{J}_a) \cdot \mathbf{E}, \tag{B17}$$

where J_a is the current in the antenna driving the system and J is the plasma current. For periodic boundary conditions, the surface term from the Poynting flux is zero.

From §2.1, we know that the order of the electric field energy is $|\delta \mathbf{E}|^2 \sim \mathcal{O}(\epsilon^2 B_0^2 v_{th_i}^2/c^2)$ and the magnetic field energy is $|\delta \mathbf{B}|^2 \sim \mathcal{O}(\epsilon^2 B_0^2)$. Thus, in the non-relativistic limit, the magnetic energy dominates and we may drop the electric field energy; this is expected since the displacement current is dropped in the non-relativistic ordering. We are left with

$$\frac{d}{dt} \int d^3 \mathbf{r} \frac{|\delta \mathbf{B}|^2}{8\pi} = -\int d^3 \mathbf{r} (\mathbf{J} + \mathbf{J}_a) \cdot \mathbf{E}.$$
 (B18)

During any growth phase, prior to saturation, both sides of the equation are of order $\mathcal{O}(\omega \epsilon^2 B_0^2) \sim \mathcal{O}(\omega \epsilon^2 n_0 T_0)$ since we have taken the plasma beta to be order unity.

Using equations (B5), (B9), and (B10) from Appendix B.1 to find the relation for $\int d^3 \mathbf{r} \mathbf{J}_s \cdot \mathbf{E}$ for each species and neglecting interspecies collisions, we obtain the equation

$$\frac{d}{dt} \int \frac{d^3 \mathbf{r}}{V} \left\{ \int d^3 \mathbf{v} \sum_{s} \left[\frac{T_{0s} h_s^2}{2F_{0s}} - q_s \phi h_s + \frac{F_{0s} q_s^2 \phi^2}{2T_{0s}} \right] + \frac{|\delta \mathbf{B}|^2}{8\pi} \right\}$$

$$= \int \frac{d^3 \mathbf{r}}{V} \int d^3 \mathbf{v} \sum_s \frac{T_{0s}}{F_{0s}} \left\langle h_s \left(\frac{\partial h_s}{\partial t} \right)_{\text{coll}} \right\rangle_{\mathbf{R}_s} - \int \frac{d^3 \mathbf{r}}{V} \mathbf{J}_a \cdot \mathbf{E}.$$
 (B19)

This equation defines energy and entropy production terms, separating out the reversible and irreversible terms. Specifically, we can define the fluctuating energy as

$$\delta E \equiv \int \frac{d^3 \mathbf{r}}{V} \left\{ \int d^3 \mathbf{v} \sum_s \left[\frac{T_{0s} h_s^2}{2F_{0s}} - q_s \phi h_s + \frac{F_{0s} q_s^2 \phi^2}{2T_{0s}} \right] + \frac{|\delta \mathbf{B}|^2}{8\pi} \right\}$$

$$= \int \frac{d^3 \mathbf{r}}{V} \left\{ \int d^3 \mathbf{v} \sum_s \left[\frac{T_{0s} \delta f_s^2}{2F_{0s}} \right] + \frac{|\delta \mathbf{B}|^2}{8\pi} \right\}$$
(B20)

and entropy production by the positive-definite collisional term, the first term on the right-hand side of equation (B19), as shown by equation (B16). In the large-scale limit, appropriate for MHD, for Alfvén waves we have $h_s \sim q_s \langle \phi \rangle_{\mathbf{R}_s} / T_{0s}$; the kinetic energy becomes the $\mathbf{E} \times \mathbf{B}$ velocity squared as expected from MHD. Averaging equation (B18) over the medium-time-scale eliminates the time derivative term, leaving the steady state balance

$$\int d^3 \mathbf{r} \overline{(\mathbf{J} + \mathbf{J}_a) \cdot \mathbf{E}} = 0.$$
 (B21)

The medium-time-scale average of equation (B19), after substituting for the collisional term in equation (B13), gives the equation for the medium-time-scale averaged energy conservation

$$\sum_{s} \frac{3}{2} n_{0s} \frac{dT_{0s}}{dt} = -\int \frac{d^3 \mathbf{r}}{V} \overline{\mathbf{J}_a \cdot \mathbf{E}}.$$
 (B22)

It is clear that the energy input from the driving antenna is dissipated as heat in the plasma species; the lesson of equation (B13) in Appendix B.1 is that this heat is produced by entropy-increasing collisions.

C. Derivation of the Linear Collisionless Dispersion Relation

The dispersion relation for a linear, collisionless gyrokinetic system is derived beginning with the set of gyrokinetic equations (25), (A24), (A25), and (A26). First, assuming the electromagnetic fields and the gyrokinetic distribution function can be expressed as plane waves, the ring averages appearing in the equations can be written as multiplications by Bessel functions. The gyrokinetic equation is then solved algebraically for the distribution function. Next, this solution for the distribution function is substituted into equations (A24), (A25), and (A26), and the integration over velocity is performed using the plasma dispersion function to simplify the parallel velocity integrals and modified Bessel functions to express

the perpendicular velocity integrals. The condition for the existence of a solution to the resulting set of algebraic equations for the electromagnetic fields is the dispersion relation. In this appendix, the plasma species subscript s is suppressed when unnecessary.

C.1. Solving for the Distribution Function

First, we decompose the electromagnetic potentials into plane wave solutions of the form $q(\mathbf{r},t) = \hat{q} \exp[i(\mathbf{k} \cdot \mathbf{r} - \omega t)]$, where q denotes χ , ϕ , or \mathbf{A} , and the gyrokinetic distribution function into solutions of the form $h(\mathbf{R}, \mathbf{v}, t) = \hat{h}(\mathbf{v}) \exp[i(\mathbf{k} \cdot \mathbf{R} - \omega t)]$. To solve equation (25) for \hat{h} , we need to express $\langle \chi \rangle_{\mathbf{R}}$ in algebraic terms. Under the plane wave decomposition, ring averages reduce to multiplications by Bessel functions. For example, the terms with the scalar potential ϕ in the definition of χ , equation (A19), yield

$$\langle \phi(\mathbf{r}, t) \rangle_{\mathbf{R}} = \hat{\phi} e^{i(\mathbf{k} \cdot \mathbf{R} - \omega t)} \frac{1}{2\pi} \oint d\theta e^{i(k_{\perp} v_{\perp}/\Omega) \cos \theta} = J_0(\frac{k_{\perp} v_{\perp}}{\Omega}) \hat{\phi}(t) e^{i(\mathbf{k} \cdot \mathbf{R} - \omega t)}.$$
 (C1)

Here we have used the definition of the zeroth-order Bessel function (Abramowitz and Stegun 1972) and the relation between the position and guiding center, equation (8), noting that $\mathbf{k} \cdot \boldsymbol{\rho} = \frac{k_{\perp} v_{\perp}}{\Omega} \cos \theta$, where θ is the angle between \mathbf{k}_{\perp} and the gyroradius $\boldsymbol{\rho}$. After further algebraic manipulations of this kind, the ring averaged potential $\langle \chi \rangle_{\mathbf{R}}$ can be written in terms of n = 0 and n = 1 Bessel functions,

$$\langle \chi \rangle_{\mathbf{R}} = \left[J_0(\frac{k_{\perp} v_{\perp}}{\Omega})(\hat{\phi} - \frac{v_{\parallel} \hat{A}_{\parallel}}{c}) + \frac{J_1(\frac{k_{\perp} v_{\perp}}{\Omega})}{\frac{k_{\perp} v_{\perp}}{\Omega}} \frac{m v_{\perp}^2}{q} \frac{\delta \hat{B}_{\parallel}}{B_0} \right] e^{i(\mathbf{k} \cdot \mathbf{R} - \omega t)}. \tag{C2}$$

where we have used the definition $\delta \hat{B}_{\parallel} = i(\mathbf{k}_{\perp} \times \hat{\mathbf{A}}_{\perp}) \cdot \hat{\mathbf{z}}$.

Similarly, the ring average of the distribution function at constant ${\bf r}$ of the distribution function becomes

$$\langle h(\mathbf{R}, v, v_{\perp}, t) \rangle_{\mathbf{r}} = J_0(\frac{k_{\perp}v_{\perp}}{\Omega})\hat{h}(v, v_{\perp})e^{i(\mathbf{k}\cdot\mathbf{r}-\omega t)}.$$
 (C3)

The linearized gyrokinetic equation can now be solved for the distribution function

$$\hat{h} = \frac{qF_0}{T_0} \frac{\omega}{\omega - k_{\parallel} v_{\parallel}} \langle \hat{\chi} \rangle_{\mathbf{R}}.$$
 (C4)

Using equation (C2), this can be written in terms of the potentials in the form

$$\hat{h} = \frac{qF_0}{T_0} \left\{ J_0 \left(\frac{k_{\perp} v_{\perp}}{\Omega} \right) \frac{\omega \hat{A}_{\parallel}}{k_{\parallel} c} + \frac{\omega}{\omega - k_{\parallel} v_{\parallel}} \left[J_0 \left(\frac{k_{\perp} v_{\perp}}{\Omega} \right) \left(\hat{\phi} - \frac{\omega \hat{A}_{\parallel}}{k_{\parallel} c} \right) + \frac{J_1 \left(\frac{k_{\perp} v_{\perp}}{\Omega} \right)}{\frac{k_{\perp} v_{\perp}}{\Omega}} \frac{m v_{\perp}^2}{q} \frac{\delta \hat{B}_{\parallel}}{B_0} \right] \right\}. \tag{C5}$$

C.2. Performing the Integration over Velocity

Because the solution for the distribution function equation (C5) is a product of functions of v_{\parallel} and v_{\perp} , the integrals over velocity space, $\int d^3\mathbf{v} = \int_0^{\infty} dv_{\parallel} \int_{-\infty}^{\infty} v_{\perp} dv_{\perp} \int_0^{2\pi} d\theta$, in equations (A24)–(A26) can be expressed in terms of plasma dispersion functions and modified Bessel functions. Hence, we can derive an algebraic set of equations for the potentials $\hat{\phi}$, \hat{A}_{\parallel} , and $\delta \hat{B}_{\parallel}$ from the quasineutrality condition equation (A24), the parallel Ampère's Law equation (A25), and the perpendicular Ampère's Law equation (A26).

Integrals over v_{\parallel} , when not immediately completed, can be written in terms of the plasma dispersion function (Fried and Conte 1961)

$$Z(\xi) = \frac{1}{\sqrt{\pi}} \int_{L} dx \frac{e^{-x^2}}{x - \xi},$$
 (C6)

where the argument is

$$\xi = \frac{\omega}{|k_{\parallel}|v_{th}} \tag{C7}$$

and the integral is performed over the Landau contour from $-\infty$ to $+\infty$ below the pole at $x = \xi$ in the complex plane.

Integrations over v_{\perp} involve pairs of Bessel functions and can be written as modified Bessel functions. Three such integrals arise in the calculation of the linear gyrokinetic dispersion relation; we label them $\Gamma_0(\alpha)$, $\Gamma_1(\alpha)$, and $\Gamma_2(\alpha)$. These integrals are

$$\Gamma_{0}(\alpha) = \int_{0}^{\infty} \frac{2v_{\perp} dv_{\perp}}{v_{th}^{2}} J_{0}^{2} \left(\frac{k_{\perp} v_{\perp}}{\Omega}\right) e^{-v_{\perp}^{2}/v_{th}^{2}} = I_{0}(\alpha) e^{-\alpha},$$

$$\Gamma_{1}(\alpha) = \int_{0}^{\infty} \frac{2v_{\perp} dv_{\perp}}{v_{th}^{2}} \frac{2v_{\perp}^{2}}{v_{th}^{2}} \frac{J_{0} \left(\frac{k_{\perp} v_{\perp}}{\Omega}\right) J_{1} \left(\frac{k_{\perp} v_{\perp}}{\Omega}\right)}{\frac{k_{\perp} v_{\perp}}{\Omega}} e^{-v_{\perp}^{2}/v_{th}^{2}} = [I_{0}(\alpha) - I_{1}(\alpha)] e^{-\alpha},$$

$$\Gamma_{2}(\alpha) = \int_{0}^{\infty} \frac{2v_{\perp} dv_{\perp}}{v_{th}^{2}} \frac{4v_{\perp}^{4}}{v_{th}^{4}} \left[\frac{J_{1} \left(\frac{k_{\perp} v_{\perp}}{\Omega}\right)}{\frac{k_{\perp} v_{\perp}}{\Omega}}\right]^{2} e^{-v_{\perp}^{2}/v_{th}^{2}} = 2\Gamma_{1}(\alpha),$$
(C8)

where I_0 and I_1 are the modified Bessel functions, the argument is $\alpha = \frac{k_{\perp}^2 \rho^2}{2}$, and we have used a relation for integrals of Bessel Functions (Watson 1966),

$$\int_{0}^{\infty} e^{-a^{2}x^{2}} J_{n}(px) J_{n}(qx) x dx = \frac{1}{2a^{2}} e^{-(p^{2}+q^{2})/(4a^{2})} I_{n}\left(\frac{pq}{2a^{2}}\right).$$
 (C9)

C.3. Quasineutrality Condition

Beginning with the gyrokinetic quasineutrality condition equation (A24), we write the ring average of the distribution function at constant position \mathbf{r} as a multiplication by a Bessel

function as in equation (C3) and substitute \hat{h} from equation (C5) into the velocity integral; the integral term then becomes

$$2\pi \int_{-\infty}^{\infty} dv_{\parallel} \int_{0}^{\infty} v_{\perp} dv_{\perp} J_{0} \left(\frac{k_{\perp} v_{\perp}}{\Omega}\right) \frac{q^{2} F_{0}}{T_{0}} \left\{ J_{0} \left(\frac{k_{\perp} v_{\perp}}{\Omega}\right) \frac{\omega \hat{A}_{\parallel}}{k_{\parallel} c} + \frac{\omega}{\omega - v_{\parallel} k_{\parallel}} \left[J_{0} \left(\frac{k_{\perp} v_{\perp}}{\Omega}\right) \left(\hat{\phi} - \frac{\omega \hat{A}_{\parallel}}{k_{\parallel} c}\right) + \frac{J_{1} \left(\frac{k_{\perp} v_{\perp}}{\Omega}\right)}{\frac{k_{\perp} v_{\perp}}{\Omega}} \frac{m v_{\perp}^{2}}{q} \frac{\delta \hat{B}_{\parallel}}{B_{0}} \right] \right\} e^{i\mathbf{k}\cdot\mathbf{r}}.$$
 (C10)

Using equation (A13) for the equilibrium distribution function F_0 , integrating over the parallel velocity using equation (C6), integrating over the perpendicular velocity using equation (C8), employing equation (C1) for the potential in the Boltzmann term of equation (A24), and summing over species yields the desired quasineutrality condition

$$\sum_{s} \frac{q_s^2 n_{0s}}{T_{0s}} \left\{ \left[1 + \Gamma_0(\alpha_s) \xi_s Z(\xi_s) \right] \left(\hat{\phi} - \frac{\omega \hat{A}_{\parallel}}{k_{\parallel} c} \right) + \left[1 - \Gamma_0(\alpha_s) \right] \left(\frac{\omega \hat{A}_{\parallel}}{k_{\parallel} c} \right) + \Gamma_1(\alpha_s) \xi_s Z(\xi_s) \left(\frac{T_{0s}}{q_s} \frac{\delta \hat{B}_{\parallel}}{B_0} \right) \right\} = 0.$$
(C11)

C.4. Parallel Ampère's Law

To perform the velocity integrals for the parallel component of Ampère's Law, it is convenient to use the linearized gyrokinetic equation (25) to find an expression for J_{\parallel} by multiplying the equation for both species by the charge, integrating over velocity, and summing over species to obtain

$$\sum_{s} \int d^{3}\mathbf{v} q_{s} \left[\frac{\partial h_{s}}{\partial t} + v_{\parallel} \frac{\partial h_{s}}{\partial z} - \frac{q_{s}}{T_{0s}} F_{0s} \frac{\partial \langle \chi \rangle_{\mathbf{R}_{s}}}{\partial t} \right] = 0.$$
 (C12)

Using charge neutrality of the equilibrium, $\sum_s n_{0s} q_s = 0$, this equation yields an expression for J_{\parallel}

$$\frac{\partial}{\partial z} J_{\parallel} = -\frac{\partial}{\partial t} \left\{ \sum_{s} \frac{q_s^2 n_{0s}}{T_{0s}} \left(\phi - \langle \langle \phi \rangle \rangle_s - \langle \langle \mathbf{v}_{\perp} \cdot \mathbf{A}_{\perp} \rangle \rangle_s \right) \right\}, \tag{C13}$$

where the double brackets denote the integration

$$\langle\langle a(\mathbf{r}, \mathbf{v}, t)\rangle\rangle_s = \int_0^\infty v_\perp dv_\perp \frac{m_s}{T_{0s}} e^{-m_s v_\perp^2/(2T_{0s})} \langle\langle a(\mathbf{r}, \mathbf{v}, t)\rangle_{\mathbf{R}_s}\rangle_{\mathbf{r}}.$$
 (C14)

Equation (C13) is the gyrokinetic version of $\nabla \cdot \mathbf{J} = 0$ —on the right hand side the ϕ terms represent the divergence of the polarization current and the \mathbf{A}_{\perp} term is the divergence of the inductive $\mathbf{E} \times \mathbf{B}$ flow. Note here that the term involving A_{\parallel} is odd in v_{\parallel} and thus

integrates to zero. Decomposing J_{\parallel} into plane waves, the parallel component of Ampère's Law demands $k_{\perp}^2 \hat{A}_{\parallel} = 4\pi/c\hat{J}_{\parallel}$. Using equation (C8) to do the perpendicular velocity integrals, equation (C13) reduces to

$$k_{\perp}^{2} \hat{A}_{\parallel} = \frac{4\pi\omega}{ck_{\parallel}} \sum_{s} \frac{q_{s}^{2} n_{0s}}{T_{0s}} \left\{ [1 - \Gamma_{0}(\alpha_{s})] \hat{\phi} - \Gamma_{1}(\alpha_{s}) \frac{T_{0s}}{q_{s}} \frac{\delta \hat{B}_{\parallel}}{B_{0}} \right\}.$$
 (C15)

Using the result from the quasineutrality condition, equation (C11), we can eliminate the $\hat{\phi}$ term to obtain the desired expression for the parallel component of Ampère's Law

$$\frac{k_{\perp}^{2}k_{\parallel}^{2}c^{2}}{4\pi\omega^{2}}\left(\frac{\omega\hat{A}_{\parallel}}{k_{\parallel}c}\right) = -\sum_{s} \frac{q_{s}^{2}n_{0s}}{T_{0s}}\left\{\Gamma_{0}(\alpha_{s})[1+\xi_{s}Z(\xi_{s})]\left(\hat{\phi} - \frac{\omega\hat{A}_{\parallel}}{k_{\parallel}c}\right) + \Gamma_{1}(\alpha_{s})[1+\xi_{s}Z(\xi_{s})]\left(\frac{T_{0s}}{q_{s}}\frac{\delta\hat{B}_{\parallel}}{B_{0}}\right)\right\}.$$
(C16)

C.5. Perpendicular Ampère's Law

Employing the plasma dispersion function, equation (C6), for the parallel velocity integrals, using equation (C8) for the perpendicular velocity integrals, summing over species, and simplifying with the definition of the cyclotron frequency and the thermal velocity, the perpendicular component of Ampère's Law, equation (A26), produces

$$-\frac{B_0^2}{4\pi} \left(\frac{\delta \hat{B}_{\parallel}}{B_0} \right) = \sum_s q_s n_{0s} \left[\Gamma_1(\alpha_s) \left(\frac{\omega \hat{A}_{\parallel}}{k_{\parallel} c} \right) - \Gamma_1(\alpha_s) \xi_s Z(\xi_s) \left(\hat{\phi} - \frac{\omega \hat{A}_{\parallel}}{k_{\parallel} c} \right) - \Gamma_2(\alpha_s) \xi_s Z(\xi_s) \left(\frac{T_{0s}}{q_s} \frac{\delta \hat{B}_{\parallel}}{B_0} \right) \right]. \tag{C17}$$

C.6. Dispersion Relation

Before combining equations to produce the dispersion relation, we specify an electron and proton plasma, allowing us to take $n_{0i} = n_{0e}$ and $q_i = -q_e = e$. Using this simplification, we can factor out n_{0i} , q_i , and T_{0i} from the sums over species s. Noting two manipulations,

$$\frac{k_{\perp}^{2}k_{\parallel}^{2}c^{2}}{4\pi\omega^{2}}\frac{T_{0i}}{q_{i}^{2}n_{0i}} = \frac{k_{\perp}^{2}\rho_{i}^{2}}{2}\frac{k_{\parallel}^{2}v_{A}^{2}}{\omega^{2}}$$
(C18)

and

$$\frac{B_0^2}{4\pi n_{0i}q_i} = \frac{2}{\beta_i} \frac{T_{0i}}{q_i},\tag{C19}$$

we can divide equations (C11) and (C16) by $q_i^2 n_{0i}/T_{0i}$ and equation (C17) by $q_i n_{0i}$ and collect like terms to yield our algebraic set of equations for $\hat{\phi} - \frac{\omega \hat{A}_{\parallel}}{k_{\parallel}c}$, $\frac{\omega \hat{A}_{\parallel}}{k_{\parallel}c}$, and $\frac{T_{0i}}{q_i} \frac{\delta \hat{B}_{\parallel}}{B}$. This system of equations can be written succinctly in matrix form as

$$\begin{pmatrix}
A & B & C \\
A - B & \alpha_i/\overline{\omega}^2 & C + E \\
C & -E & D - 2/\beta_i
\end{pmatrix}
\begin{pmatrix}
\hat{\phi} - \frac{\omega \hat{A}_{\parallel}}{k_{\parallel}c} \\
\frac{\omega \hat{A}_{\parallel}}{k_{\parallel}c} \\
\frac{T_{0i}}{q_i} \frac{\delta \hat{B}_{\parallel}}{B}
\end{pmatrix} = 0,$$
(C20)

where we have used the definitions already given in equations (27-34). Setting the determinant of this matrix equal to zero gives the dispersion relation for linear, collisionless gyrokinetics

$$\left[\frac{\alpha_i A}{\overline{\omega}^2} - AB + B^2\right] \left[\frac{2A}{\beta_i} - AD + C^2\right] = \left[AE + BC\right]^2. \tag{C21}$$

The physical interpretation of this dispersion relation is simple: the left-hand side of equation (C21) contains two factors, the first corresponding to the Alfvén wave solution and the second to the slow wave solution; the right-hand side represents a finite Larmor radius coupling between the Alfvén and slow waves that occurs as $k_{\perp}\rho_i$ approaches unity.

D. Analytical Limits of the Dispersion Relation

The linear, collisionless dispersion relation equation (26) harbors the plasma dispersion functions $Z(\xi_s)$ and the integrals of the Bessel functions over the perpendicular velocity $\Gamma_0(\alpha_s)$, $\Gamma_{1s}(\alpha_s)$, and $\Gamma_2(\alpha_s)$; these functions can be approximated by simple analytical series for large and small arguments, allowing an analytical form of the dispersion relation to be derived in these limits. The arguments of the plasma dispersion function are $\xi_i = \overline{\omega}/\sqrt{\beta_i}$ and $\xi_e = \overline{\omega}/\sqrt{\beta_e} = (m_e/m_i)^{1/2}(T_{0i}/T_{0e})^{1/2}\overline{\omega}/\sqrt{\beta_i}$; for the perpendicular velocity integrals, they are $\alpha_i = (k_\perp \rho_i)^2/2$ and $\alpha_e = (k_\perp \rho_e)^2/2 = (m_e/m_i)(T_{0e}/T_{0i})(k_\perp \rho_i)^2/2$. Thus, the natural subsidiary expansion parameters in the dispersion relation are α_i , $\sqrt{\beta_i}$, and $(T_{0i}/T_{0e})^{1/2}$. The limit of large scale, $\alpha_i \ll 1$, discussed in §2.5, illuminates the physical meaning of each of the terms of the dispersion relation through a connection to the well-known MHD Alfvén and slow modes. In this appendix, we examine the behavior of the Alfvén mode in the limits of high beta $\sqrt{\beta_i} \gg 1$, and low beta $\sqrt{\beta_i} \ll 1$. We consider only the Alfvén mode because, as discussed in §2.6, we expect the turbulent cascade to be almost entirely Alfvénic in character since the slow wave is damped on scales below the mean free path.

D.1. High Beta Limit, $\sqrt{\beta_i} \gg 1$

In the high beta limit, we make two asymptotic expansions: one for $k_{\perp}\rho_i \sim \mathcal{O}(\beta_i^{-1/4})$ and another for $k_{\perp}\rho_i \sim \mathcal{O}(1)$. For both of these expansions, the plasma dispersion functions can be expanded for small arguments since $\sqrt{\beta_i} \gg 1$ and we assume $(T_{0i}/T_{0e})^{1/2} \ll (m_i/m_e)^{1/2}\sqrt{\beta_i}$.

For $k_{\perp}\rho_i \sim \mathcal{O}(\beta_i^{-1/4})$, we will find that $\overline{\omega} \sim \mathcal{O}(1)$. In this limit, we can use the small argument limit of the perpendicular velocity integrals equation (C8) to find the order of the dispersion relation coefficients $B \sim \mathcal{O}(\beta_i^{-1/2})$ and $E \sim \mathcal{O}(\beta_i^{-1/2})$. Keeping only terms of order $\mathcal{O}(\beta_i^{-1})$, the dispersion relation simplifies to

$$\alpha_i D(\overline{\omega}^2 - 1) = \frac{9}{4} \overline{\omega}^2 \alpha_i^2. \tag{D1}$$

We can write $D = i\sqrt{\pi}G_1\frac{\overline{\omega}}{\sqrt{\beta_i}}$, where $G_1 = 2[\Gamma_{1i} + (m_e/m_i)^{1/2}]$. Solving for $\overline{\omega}$ yields

$$\overline{\omega} = -i\frac{9\alpha_i}{4G_1}\sqrt{\frac{\beta_i}{\pi}} \pm \sqrt{1 - \frac{81\beta_i\alpha_i^2}{64\pi G_1}}.$$
 (D2)

In the limit $k_{\perp}\rho_i \ll \beta_i^{-1/4}$, we recover the expected Alfvén wave with weak damping, $\overline{\omega} = 1 - i \frac{9\alpha_i}{4G_1} \sqrt{\frac{\beta_i}{\pi}}$; this verifies our assumption that $\overline{\omega} \sim \mathcal{O}(1)$. For $\alpha_i > (8G_1/9)\sqrt{\pi/\beta_i}$, the frequency is purely imaginary, with the solution in the overlap region $\beta_i^{-1/4} \ll k_{\perp}\rho_i \ll 1$ given by

$$\overline{\omega} = -i\frac{4G_1}{9\alpha_i}\sqrt{\frac{\pi}{\beta_i}}.$$
 (D3)

In the limit $k_{\perp}\rho_i \gtrsim 1$, we will find that $\overline{\omega} \sim \mathcal{O}(\beta_i^{-1/2})$. Keeping only terms of order $\mathcal{O}(1)$, the dispersion relation reduces to

$$\overline{\omega}^2 \beta_i E^2 + \alpha_i \beta_i D - 2\alpha_i = 0. \tag{D4}$$

Solving for the frequency produces the result

$$\overline{\omega} = -i\frac{\alpha_i G_1}{2E^2} \sqrt{\frac{\pi}{\beta_i}} \pm \sqrt{\frac{2\alpha_i}{\beta_i E^2} - \frac{\alpha_i^2 G_1^2 \pi}{4E^4 \beta_i}}.$$
 (D5)

This solution confirms our assumption that $\overline{\omega} \sim \mathcal{O}(\beta_i^{-1/2})$. In the limit $k_{\perp}\rho_i \ll 1$, this solution reproduces equation (D3), demonstrating that these two asymptotic expansions match in the overlap region. Plots of the real frequency and damping rate for $\beta_i = 100$ and $T_{0i}/T_{0e} = 100$ given by both solutions, including the overlap region where the solution is purely imaginary, are presented in Figure 9.

D.2. Low Beta Limit, $\sqrt{\beta_i} \ll 1$

In the low beta limit $\sqrt{\beta_i} \ll 1$, the argument of the ion plasma dispersion function ξ_i is large, but the argument for the electron plasma dispersion function ξ_e depends on the size the electron plasma beta β_e , or if the ion plasma beta β_i has been specified, on the temperature ratio T_{0i}/T_{0e} . We consider the cases of small and large ξ_e separately.

For $(T_{0i}/T_{0e})^{1/2} \gg 1$ (or $\beta_e \ll 1$), the dispersion relation, equation (26), in the lowest nontrivial order, reduces to

$$\left[\frac{\alpha_i}{\overline{\omega}^2} - B + \frac{B^2}{A}\right] \left[\frac{2}{\beta_i} - D\right] A = 0.$$
 (D6)

Focusing on the first factor, which corresponds to the Alfvén wave solutions, gives us the dispersion relation

$$\frac{B}{2\overline{\omega}^2}(2\alpha_i + \beta_i Q) - \frac{\alpha_i \beta_i Q}{2\overline{\omega}^4} + i\sqrt{\frac{\pi}{\beta_i}} \frac{P(\overline{\omega})}{\overline{\omega}} (\alpha_i - \overline{\omega}^2 B), \tag{D7}$$

where

$$Q = \Gamma_{0i} - \frac{m_i}{m_e} \Gamma_{0e} \tag{D8}$$

and

$$P(\overline{\omega}) = \Gamma_{0i} \exp\left(-\frac{\overline{\omega}^2}{\beta_i}\right) + \Gamma_{0e} \left(\frac{m_e}{m_i}\right)^{1/2} \left(\frac{T_{0i}}{T_{0e}}\right)^{3/2} \exp\left(-\frac{m_e T_{0i}}{m_i T_{0e}} \frac{\overline{\omega}^2}{\beta_i}\right). \tag{D9}$$

Assuming weak damping, we can solve by Taylor expanding about the real frequency (Krall and Trivelpiece 1986) to determine the solution

$$\overline{\omega}^2 = \frac{\alpha_i \beta_i Q}{(2\alpha_i + \beta_i Q)B} \tag{D10}$$

and

$$\overline{\gamma} = \frac{-\sqrt{\frac{\pi}{\beta_i}}\overline{\omega}^4(\alpha_i - \overline{\omega}^2 B)P(\overline{\omega})}{\alpha_i\beta_i Q}.$$
 (D11)

For $(T_{0i}/T_{0e})^{1/2} \ll 1$ (or $\beta_e \gg 1$), the dispersion relation, equation (26), in the lowest nontrivial order, again reduces to equation (D6). Following the same procedure as above, the dispersion relation in this limit simplifies to

$$\overline{\omega}^4 L + \overline{\omega}^2 M + N = 0, \tag{D12}$$

where

$$L = \frac{T_{0i}}{T_{0e}} \Gamma_{0e} B, \tag{D13}$$

$$M = \alpha_i B + \alpha_i \frac{T_{0i}}{T_{0e}} \Gamma_{0e} + \frac{\beta_i \Gamma_{0i} B}{2}$$
(D14)

and

$$N = \frac{\alpha_i \beta_i \Gamma_{0i}}{2}.$$
 (D15)

Assuming again weak damping, the solution is found to be

$$\overline{\omega}^2 = \frac{M \pm \sqrt{M^2 - 4NL}}{2L} \tag{D16}$$

and

$$\overline{\gamma} = \frac{-\sqrt{\frac{\pi}{\beta_i}}\overline{\omega}^4(\alpha_i - \overline{\omega}^2 B) \left[\Gamma_{0i} \exp\left(-\frac{\overline{\omega}^2}{\beta_i}\right) + \Gamma_{0e} \left(\frac{m_e}{m_i}\right)^{1/2} \left(\frac{T_{0i}}{T_{0e}}\right)^{3/2}\right]}{2(2N - \overline{\omega}^2 M)}.$$
 (D17)

Both of the low beta limit solutions, for $(T_{0i}/T_{0e})^{1/2} \gg 1$ and $(T_{0i}/T_{0e})^{1/2} \ll 1$ (with the plus sign), are plotted against numerical solutions of the full dispersion relation in Figure 10.

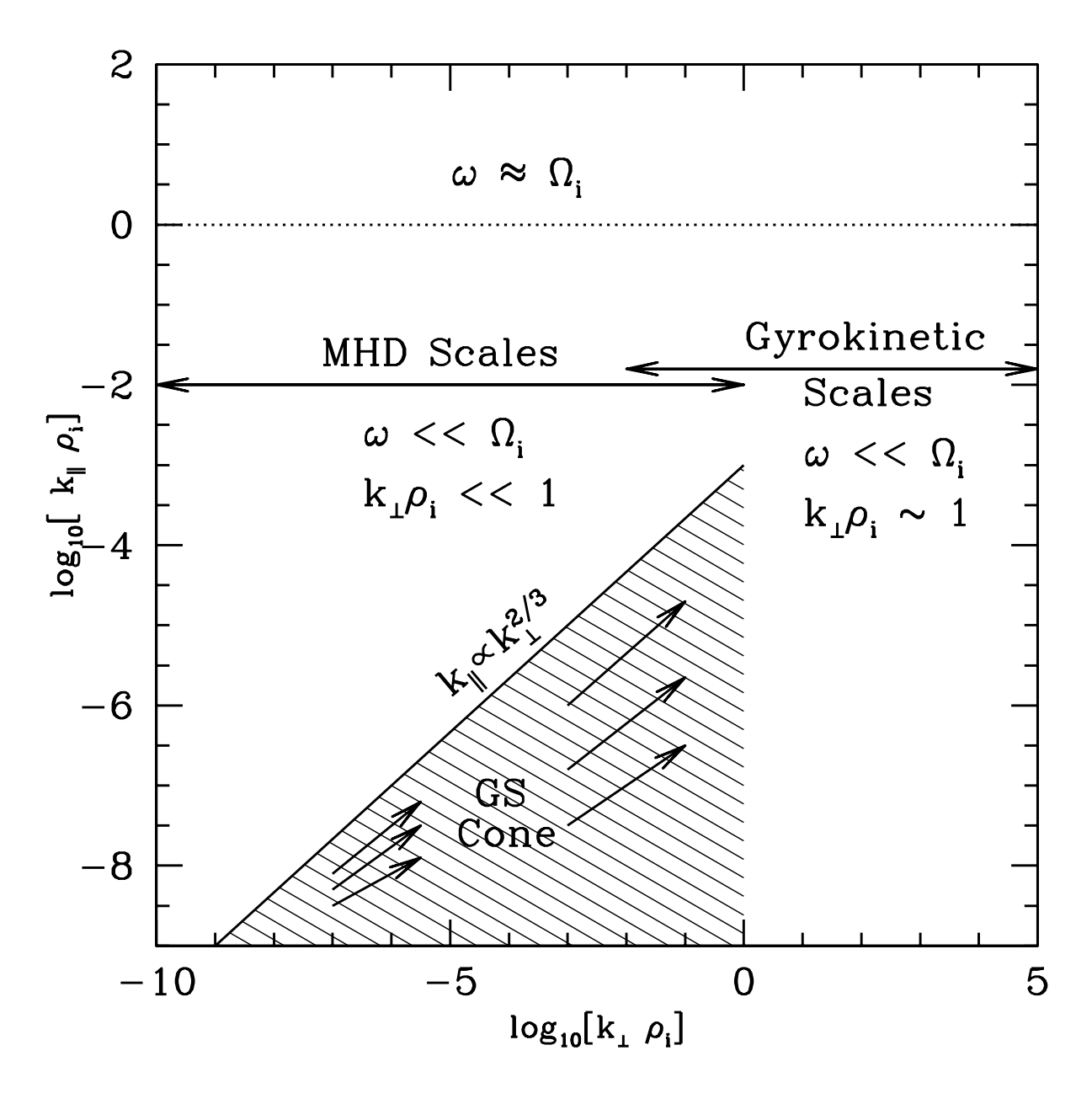


Fig. 1.— Schematic diagram highlighting the anisotropic character of magnetized turbulence as described by the theory of Goldreich and Sridhar (1995). MHD (or, rather, strictly speaking, its Alfvén-wave part; see Schekochihin et al. 2006) is formally valid only in the limit that $\omega \ll \Omega_i$ and $k_{\perp}\rho_i \ll 1$; gyrokinetic theory remains valid when the perpendicular wavenumber is of the order of the ion Larmor radius, $k_{\perp}\rho_i \sim 1$. Note that the fluctuation frequency ω approaches the ion cyclotron frequency Ω_i when $k_{\parallel}\rho_i \to 1$, so the parameter space where gyrokinetics is applicable can also be described as $k_{\parallel} \ll k_{\perp}$. Hence, the anisotropic turbulence of GS theory is well described by gyrokinetics.

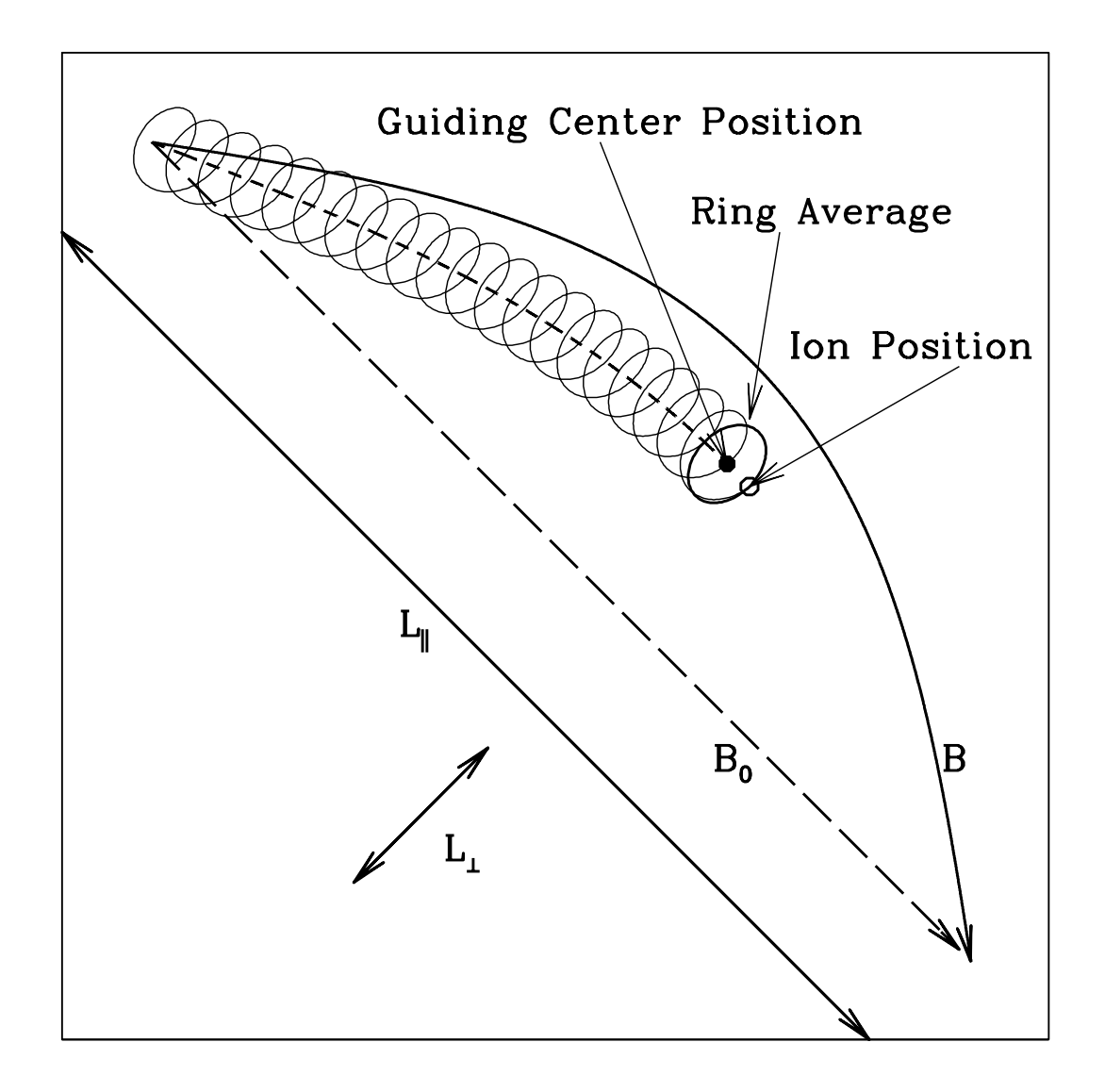


Fig. 2.— Diagram illustrating the ring average in gyrokinetics. The ion position is given by the open circle, the guiding center position by the filled circle; the ring average, centered on the guiding center position, is denoted by the thick-lined circle passing through the particle's position. The characteristic perpendicular and parallel length scales in gyrokinetics are marked L_{\perp} and L_{\parallel} ; here the perpendicular scale is exaggerated for clarity. The unperturbed magnetic field ${\bf B}_0$ is given by the long-dashed line and the perturbed magnetic field ${\bf B}$ by the solid line.

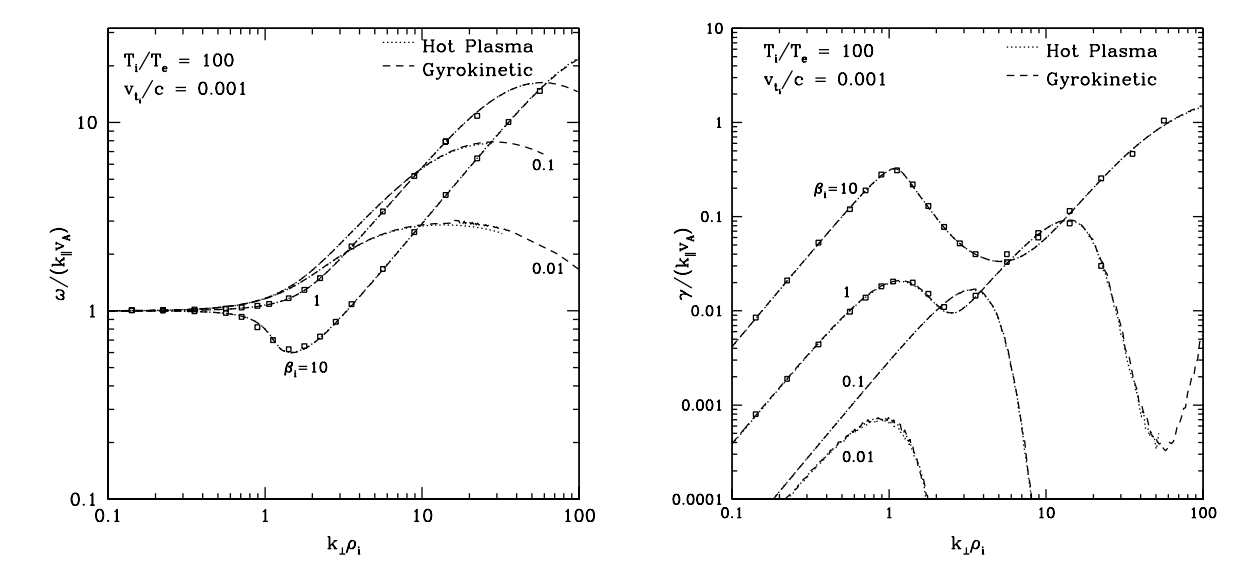


Fig. 3.— The normalized real frequency $\omega/(k_{\parallel}v_A)$ (left) and damping rate $\gamma/(k_{\parallel}v_A)$ (right) vs. $k_{\perp}\rho_i$ for a temperature ratio $T_{0i}/T_{0e}=100$ over the range of ion plasma beta values $\beta_i=10,1,0.1,0.01$. Plotted are numerical solutions to the gyrokinetic dispersion relation (dashed lines), numerical solutions to the hot plasma dispersion relation (dotted lines), and results from the GS2 gyrokinetic code (open squares).

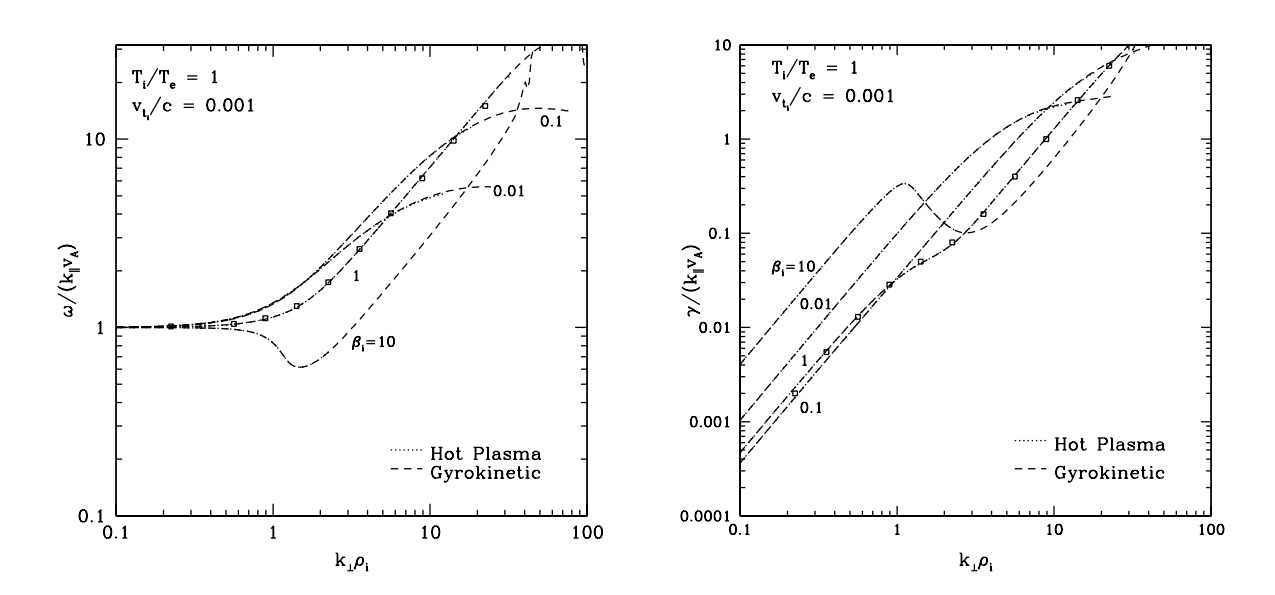


Fig. 4.— Same as Figure 3, but for $T_{0i}/T_{0e} = 1$.

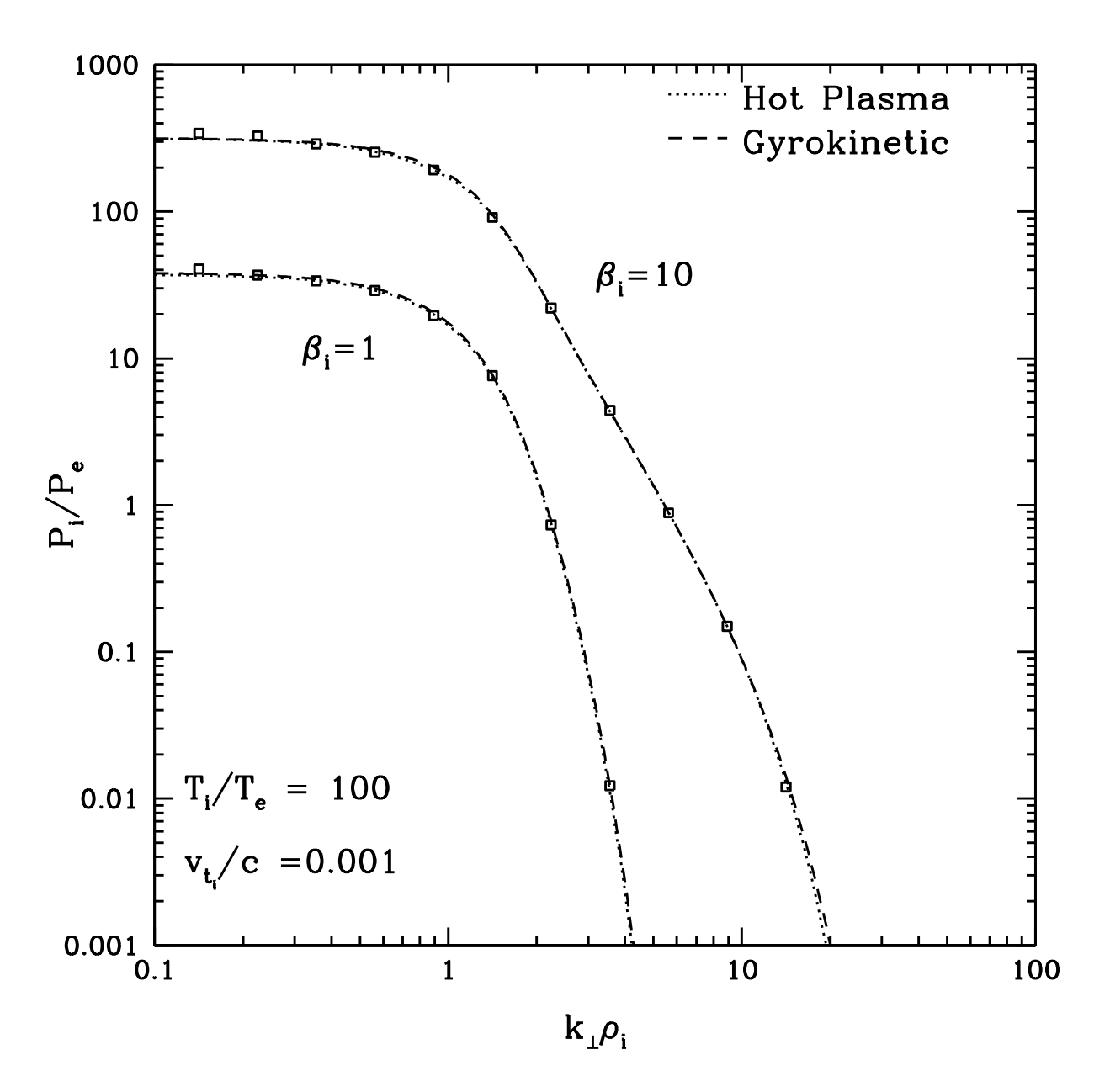


Fig. 5.— Ratio of the ion to electron heating P_i/P_e . Results are shown for a temperature ratio of $T_{0i}/T_{0e} = 100$ and values of ion plasma beta $\beta_i = 1, 10$. Plotted are derived values using the gyrokinetic dispersion relation (dashed lines) and the hot plasma dispersion relation (dotted lines); results from the GS2 gyrokinetic initial value code show good agreement over nearly five orders of magnitude (open squares).

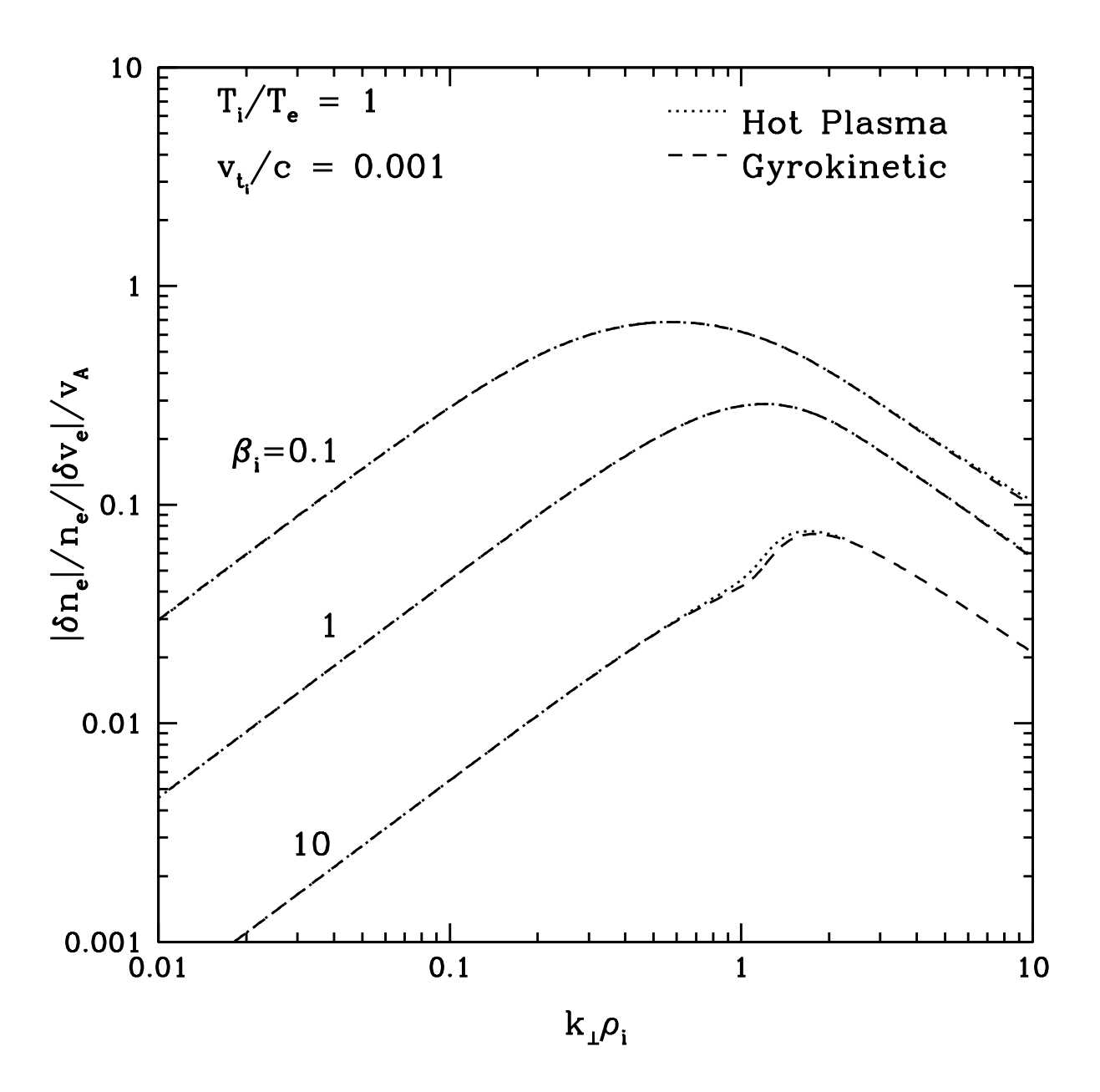


Fig. 6.— Electron density fluctuations for a plasma with a temperature ratio of $T_{0i}/T_{0e} = 1$ and values of ion plasma beta $\beta_i = 0.1$, 1, and 10 using the gyrokinetic dispersion relation (dashed lines) and the hot plasma dispersion relation (dotted lines). The fractional electron density fluctuation $|\delta n_e|/n_{0e}$ is normalized here by the total electron velocity fluctuations over the Alfvén speed $|\delta v_e|/v_A$; we see the density fluctuations peak at the scale of the ion Larmor radius.

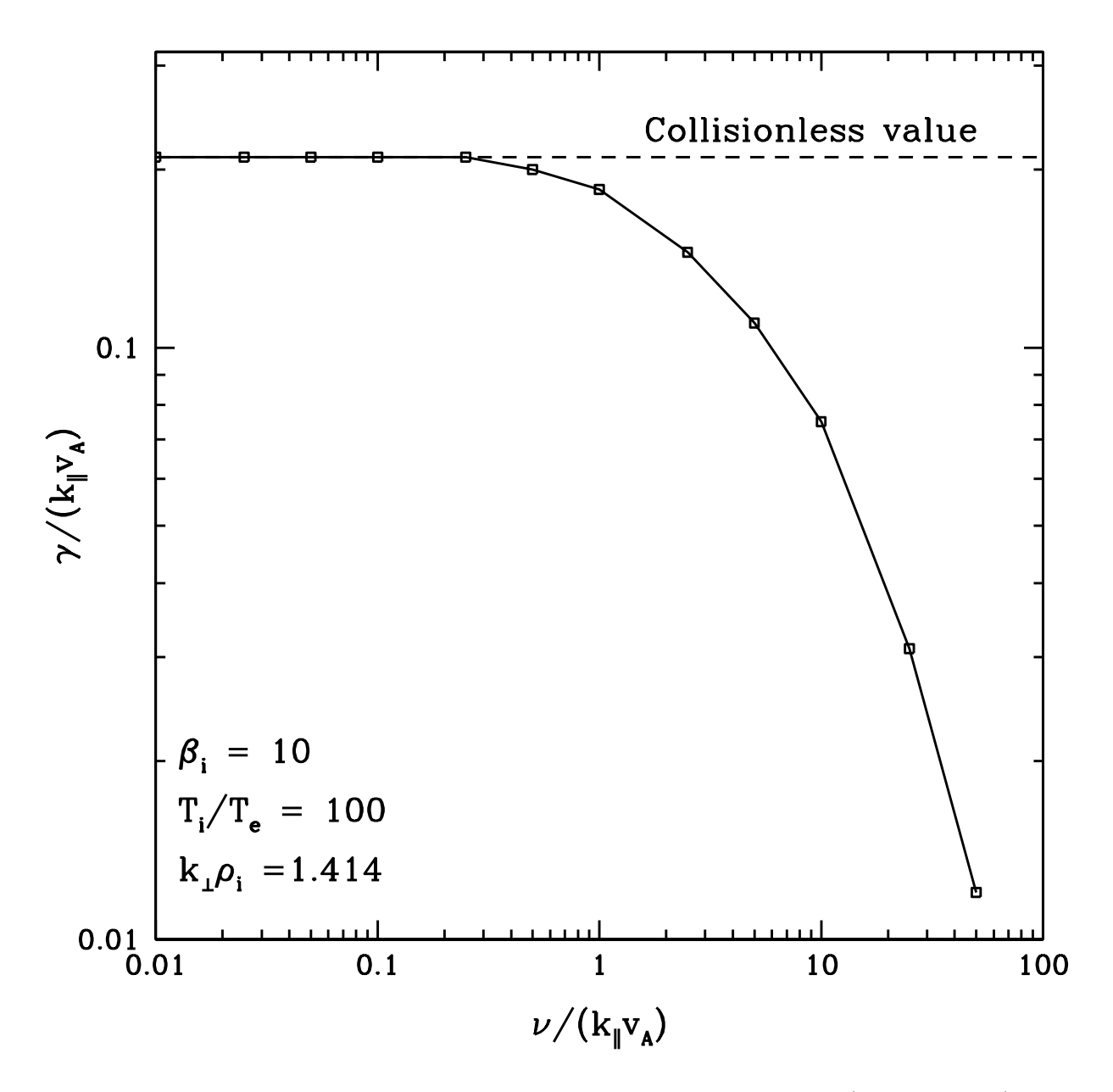


Fig. 7.— Plot of the damping rate γ determined in linear runs of GS2 (open squares) vs. the collision rate ν normalized by $k_{\parallel}v_A$. In the collisionless limit, $\nu \ll \omega$, the damping rate is independent of the collision rate as expected. As the collision rate is increased, collisionless processes for damping the wave are less effective and the damping rate diminishes.

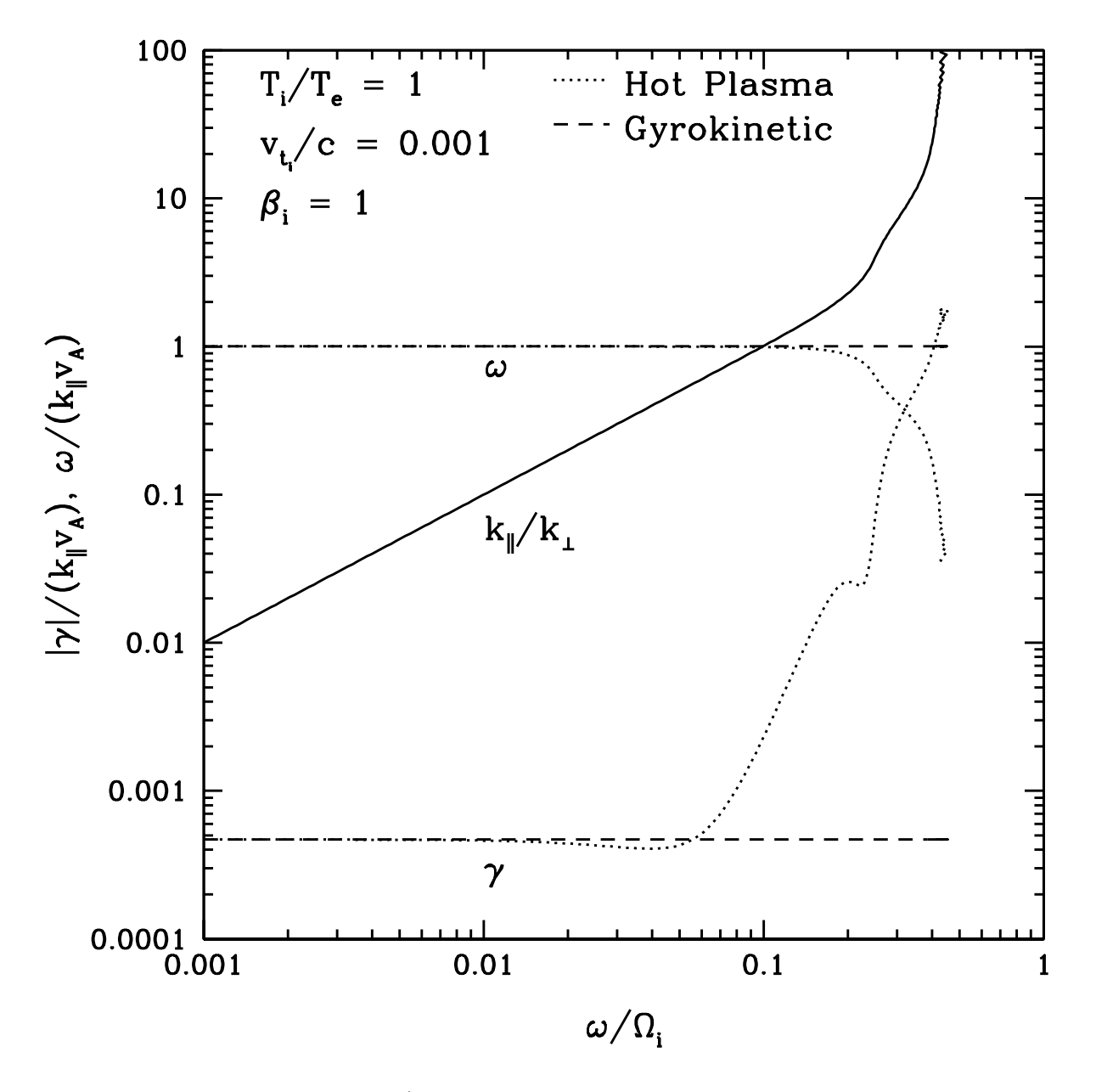


Fig. 8.— For a plasma with $T_{0i}/T_{0e}=1$, $\beta_i=1$, and $k_\perp\rho_i=0.1$, the limits of applicability of the gyrokinetic solution (dashed line) are shown as the latter deviates from the hot plasma theory solution (dashed line) when $\omega/\Omega_i \to 1$. Also plotted (solid line) is the value of k_\parallel/k_\perp as a function of ω/Ω_i .

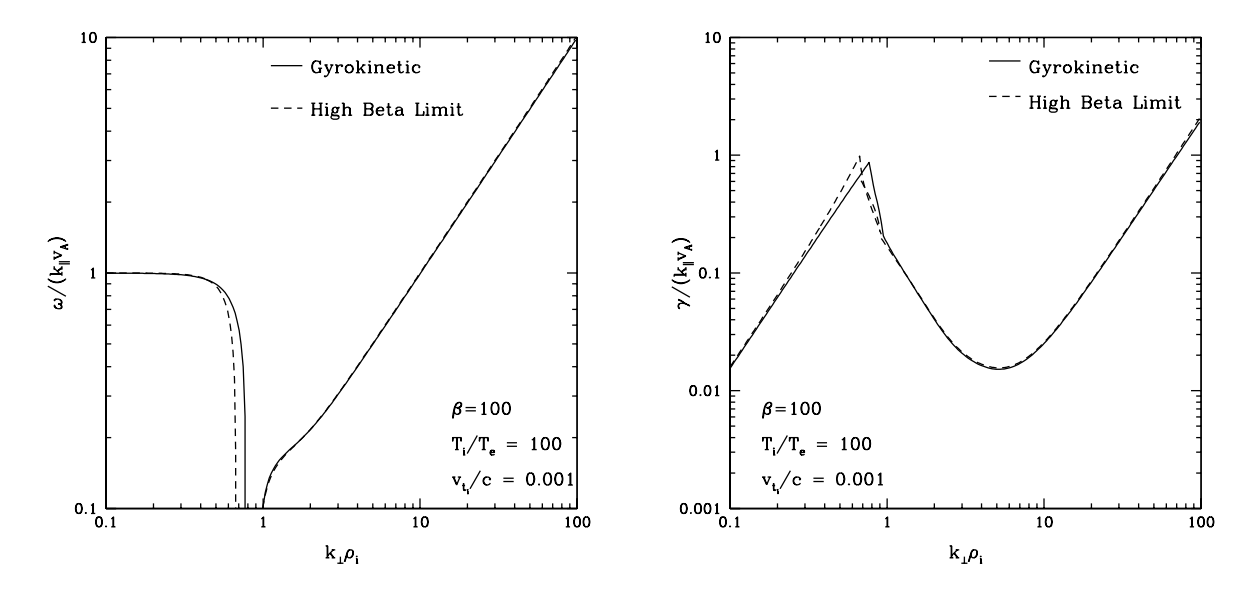


Fig. 9.— The real frequency (left) and damping rate (right) of the Alfvén solution derived by numerical solution of the linear, collisionless gyrokinetic dispersion relation (solid line) compared to the high beta analytical limit (dashed line) for $\sqrt{\beta_i} \gg 1$ and $(T_{0i}/T_{0e})^{1/2} \ll (m_i/m_e)^{1/2}\sqrt{\beta_i}$. The approximate solution consists of two solutions, valid for $k_{\perp}\rho_i \sim \mathcal{O}(\beta_i^{-1/4})$ and $k_{\perp}\rho_i \sim \mathcal{O}(1)$. In the overlap region $\beta_i^{-1/4} \ll k_{\perp}\rho_i \ll 1$, both solutions are plotted to confirm that they match.

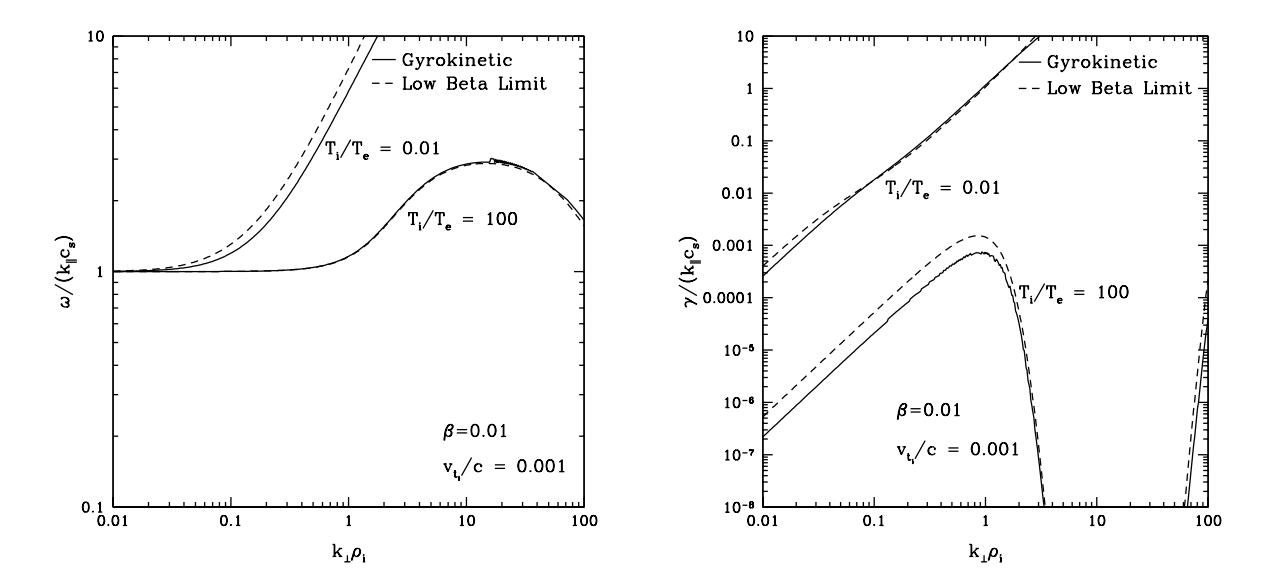


Fig. 10.— The real frequency (left) and damping rate (right) of the Alfvén solution derived by numerical solution of the linear, collisionless gyrokinetic dispersion relation (solid line) compared to the low beta analytical limit $\sqrt{\beta_i} \ll 1$ (dashed line) for $(T_{0i}/T_{0e})^{1/2} \ll 1$ and $(T_{0i}/T_{0e})^{1/2} \gg 1$.